Examining Forces at Geosynchronous Orbit with Uncontrolled Galaxy 15 Wide Area Augmentation System Ephemerides

by

David P. Schafer

A Report Submitted to the Faculty of the

Milwaukee School of Engineering

In Fulfillment of the

Requirements for the Degree of

Master of Science in Engineering

Milwaukee, Wisconsin
March 2017

ABSTRACT

In April of 2010, control of cable communications satellite Galaxy 15 was lost. The satellite remained uncontrolled, drifting in free orbit, for over nine months before control was resumed. During its drift, Galaxy 15 continued to transmit position data. These drift position data offer a unique opportunity to investigate the forces in the geostationary orbit regime. The purpose of the project that is described in this report was to compare the empirical data from Galaxy 15's uncontrolled period with a high-fidelity geosynchronous orbit dynamic model. The dynamic model was constructed with Matlab ®, and was verified by use of the satellite's ephemerides over a full month of propagation data. The model was then run for each perturbation force, simulated separately, in order to find the specific effects of each perturbation force. The project report contains an analysis of the forces, and a conclusion concerning how each force affects the orbit regime. Each force examined is found to have a large effect in at least one classical direction.

ACKNOWLEDGMENTS

I would like to express my sincere gratitude to Dr. Jill Seubert for her extensive assistance in the completion of this project. She formulated the problem this project seeks to solve, and the successful completion was only possibly through use of equations she had previously derived (published under the name Tombasco) and made available to myself. Without Dr. Seubert's immense assistance, I would not have completed this project.

I would also like to thank Prof. Gary Shimek for his fantastic technical writing assistance and his guidance on which areas of my project to focus on.

Finally, I would like to thank Dr. Kumpaty for putting my excellent team of advisors together, and pushing me to work on a project I knew I would enjoy, instead of one I already knew how to complete.

CONTENTS

LIST OF FIGURES

LIST OF TABLES

NOMENCLATURE

Symbols

A – Ideal geosynchronous radius, 42,164,200 meters

A_s – The surface area of the satellite

a – Semi-major axis

$\vec{a}$ – Perturbing acceleration vector

a_h – Disturbing acceleration in satellite body-fixed out-of-plane direction

a_r – Disturbing acceleration in satellite body-fixed radial direction

$\vec{a}_{sr}$ – Acceleration due to solar radiation pressure

a_ϕ – Disturbing acceleration in satellite body-fixed tangential direction

$\Delta\bar{a}$ – Normalized semi-major axis offset, also known as the Longitudinal drift rate

C – Computed gravitational harmonic coefficient

c_R – The reflectivity of the spacecraft surface facing the sun

$\vec{e}$ – Eccentricity vector, made up of X, Y, and Z components

e_x – X direction eccentricity variable

e_y – Y direction eccentricity variable

$\vec{F}$ – Force vector

G – The Greenwich Meridian

h – Angular momentum

$\hat{h}$ – North in LVLH frame

$\vec{\imath}$ – Inclination vector, made up of X, Y, and Z components

i_x – X direction inclination variable

$\hat{\imath}_x$ – Unit vector along X direction

i_y – Y direction inclination variable

$\hat{\imath}_y$ – Unit vector along Y direction

$\hat{\imath}_z$ – Unit vector along Z direction

$\hat{I}$ – Vector pointing from Earth center to Greenwich Meridian in ECEF reference frame

$\hat{J}$ – Vector pointing from Earth center to 90º East of Greenwich Meridian in ECEF frame

$\hat{K}$ – Vector pointing from Earth center to north in ECEF frame

m – Mass of satellite

$\vec{n}$ – Vector pointing from orbit center to the ascending node

N – Nutation matrix

p – The semilatus rectum

P – Legendre polynomial

P – Precession matrix

p_{sr} – The average pressure from the Sun at 1 AU

r – Radial distance of orbit, measured from Earth center

$\vec{r}$ – Position vector of satellite relative to Earth center

$\vec{r}_{ECEF}$ – Vector to the object of interest in the ECEF frame

$\vec{r}_{ECI}$ – Vector to the object of interest in the ECI frame

$\vec{r}_{GCRF}$ – Vector to the object of interest in the geocentric reference frame

$\vec{r}_{ITRF}$ – Vector to the object of interest in the international terrestrial reference frame

$\vec{r}_{LVLH}$ – Vector to the object of interest in the LVLH frame

R – The Earth's mean equatorial radius, roughly 6,378,100 meters

R – Sidereal rotation matrix

s – Sidereal angle

S – Computed gravitational harmonic coefficient

t – Time

U – Gravity potential

V – Velocity magnitude

$\vec{V}$ – Velocity vector

V_t – Velocity component in tangential direction

V_r – Velocity component in radial direction

V_o – Velocity component in orthogonal direction

W – Polar motion matrix

X – Inertial coordinate direction pointing towards the vernal equinox

x – Variable distance along $\hat{\imath}_x$ unit vector

Y – Inertial coordinate direction orthogonal to X in the equatorial plane

y – Variable distance along $\hat{\imath}_y$ unit vector

Z – Inertial coordinate direction orthogonal to X and Y, representing North

z – Variable distance along $\hat{\imath}_z$ unit vector

ε – The reflectivity coefficient of the spacecraft surface

λ – Geocentric longitude

μ – Gravitational parameter

ν – True anomaly

ξ – Specific mechanical energy

Π – Legendre polynomial normalizing function

σ – The effective cross-sectional area to mass ratio

φ – Uniform angular velocity

ϕ – Geocentric latitude

Ω – Right ascension of the ascending node

ω – Argument of perigee

ω_E – Rotational angular velocity of the Earth

Abbreviations

COE – Classical Orbital Elements

ECEF – Earth-Centered Earth-Fixed reference frame

ECI – Earth-Centered Inertial reference frame

GEO – Geostationary Orbit or Geosynchronous Orbit

GPS – Global Position System

LEO – Low Earth Orbit

LVLH – Local Vertical Local Horizontal satellite reference frame

WAAS – Wide Area Augmentation System

GLOSSARY

Eccentricity – Measure of how circular an orbit is. An eccentricity of zero is perfectly circular, of one is parabolic, and of greater than one is hyperbolic.

Ecliptic plane – Plane in which Earth orbits the Sun.

Ephemerides – Position and velocity coordinates for celestial bodies.

Equatorial plane – Plane coincident with Earth's equator.

Geostationary Orbit – A geosynchronous orbit in the equatorial plane that stays above the same point on the Earth for its full orbit.

Geosynchronous Orbit – An orbit around Earth that matches the revolution period of Earth.

Inclination – Angular difference between the orbit plane and the equatorial plane.

Mean Equatorial Geocentric System of Date (MEGSD) Coordinate System – A nearly inertial coordinate system from the point of view of the non-rotating center of the Earth in the orbit plane of the satellite. The Earth revolves around this center, and the distance to the satellite is measured from the mean sea level. This coordinate system differs from an inertial one by not including the precession or nutation effects of the Earth in order to vastly simplify the calculations with minimal loss of coherence.

Non-Spherical Harmonics – Model of the gravitational pull of the Earth due to its non-spherical nature.

Spacecraft-oriented Coordinate System – A non-inertial coordinate system that uses the spacecraft center of mass as the central point. This relates the directions of motion of the spacecraft to the directions of the Earth as given in MEGSD.

Subscripts 1 and 2 refer to the Sun and the Moon, respectively.

INTRODUCTION

This Master of Science in Engineering Capstone project seeks to assess theoretical geosynchronous (GEO) satellite orbital drift compared to the empirical orbital data obtained from Galaxy 15's uncontrolled period. Galaxy 15's unique history allows the chance to validate GEO long-period orbit propagations with high-accuracy empirical data of an uncontrolled object. Satellites in GEO all have specific mission parameters, and therefore, they need to hold position with high accuracy. Thus, no high-fidelity data have been previously analyzed with respect to long periods of uncontrolled satellite movement at this particular orbit, as previously no such data existed.

High-fidelity empirical ephemeris of the satellite path as it drifted is available due to the data generated by the Wide Area Augmentation System (WAAS) data systems on board and in use on the Galaxy 15 satellite. These data can be used to create a very accurate picture of specifically *where* the satellite was at any point in time over its nearly nine-month drift. Modeling a satellite in GEO includes the development of highly accurate models of the gravitation wells of the Earth, Moon, and Sun, as well as an accurate account for the solar pressure acting on the satellite's surface [1]. The solar pressure component requires an accurate model of the satellite as well as accurate attitude data from the satellite [1]. However, attitude data are not publicly available, and the satellite itself is quite complex to properly model. To solve these problems, assumptions concerning the attitude and shape of the satellite were used in this project in order to approximate the forces, so that the focus could be placed on the novel method of examining the forces.

Background

Today, thousands of known satellites encircle the globe, many of which send communications data from one point to another on this planet, with a few sending and receiving signals outwards [2]. All of these satellites have specific orbit paths to ensure proper connections and to minimize interference between connections and other satellites. Of these communication satellite orbits, by far the most popular is the *geosynchronous* orbit, or the orbit which allows a satellite to be sitting over a specific equatorial longitude as long as it maintains this orbit [3]. This means the satellite must be moving at the same angular velocity of the surface of the Earth. As orbiting body speeds are determined primarily by the radius of the orbit, geosynchronous orbits are all at the same mean radius. This simplification ignores the eccentricity of the orbit, and assumes the orbit is nearly perfectly circular. Finally, the only way to keep a satellite fixed relative to a point on the Earth's surface, is to keep it at the equator. Holding the orbit at the equator makes the geosynchronous orbit very nearly geostationary, as the satellite will remain almost stationary relative to the Earth. With all of these limitations, the only variable these geostationary satellites have any control over is their longitude. Each satellite in geostationary orbit approximately sits in a line of other satellites moving at the same speed in the same direction about 35,800 km above the equator [3].

In order to maintain a geosynchronous orbit, small adjustment maneuvers are required. Perturbations from the orbit can be caused by gravitational forces from the Sun, the Moon, and other celestial bodies, or from solar radiation off of the Sun, or even from solar wind caught in the satellite's solar panels [1]. Other sources of perturbative forces

include Earth's magnetic field and the non-homogenous (non-spherical) nature of the

Earth's mass, which affects the Earth's gravitation. All of these perturbations can throw

the satellites off of their orbits. These orbits, tracked from the ground and maintained

through several different tracking and sensing mechanisms, need to utilize the data

obtained to counteract the perturbations to keep the satellites near their ideal orbits.

Additionally, the satellites must constantly be pointed in the proper direction to maintain

data communications, as well as to keep the solar panels pointed towards the Sun,

throughout the orbits. This requires a complex set of reaction wheels, moment wheels,

mass expulsion devices (rockets), and other control systems to keep the satellites orbiting

properly and pointed in the proper directions. These further require accelerometers, star

trackers, and other sensors in order for the satellites to find what attitude corrections are

necessary. Finally, all of these systems require power. Power is usually generated from

solar panels, with some amount of battery storage onboard.

Most satellites employ onboard computers, which keep track of all of the attitude

information, and transmit it all to a ground control station, which keeps track of all the

satellites and ensures, among other things, that none of the satellites are about to collide.

Additionally, some ground stations track the satellites themselves, using radar or optical

systems to verify position [4]. Figures 1 and 2 display common coordinate systems,

which track the satellite relative to the Earth-oriented or the satellite-oriented coordinate

systems, respectively [1], and which will be used in this particular study. The Mean

Equatorial Geocentric System of Date (MEGSD) coordinate system tracks both the

satellite moving around the Earth and the rotation of the Earth. The Greenwich angle, G,

tracks the sidereal angle of the Greenwich Meridian, or the 0° longitude on Earth. λ is the

longitudinal angle from the Greenwich Meridian to the spacecraft, and the sidereal angle

s is the combination of the two from the semi-inertial reference. ω_E is the rotational

angular velocity at which the Earth rotates, r is the radius at which the satellite orbits, and

V is the tangential velocity of the spacecraft. Here, X and Y are directions in the

equatorial orbit plane that are orthogonal to each other and represent a snapshot of

directions for the rotation of the Earth; the X-axis points towards the vernal equinox.
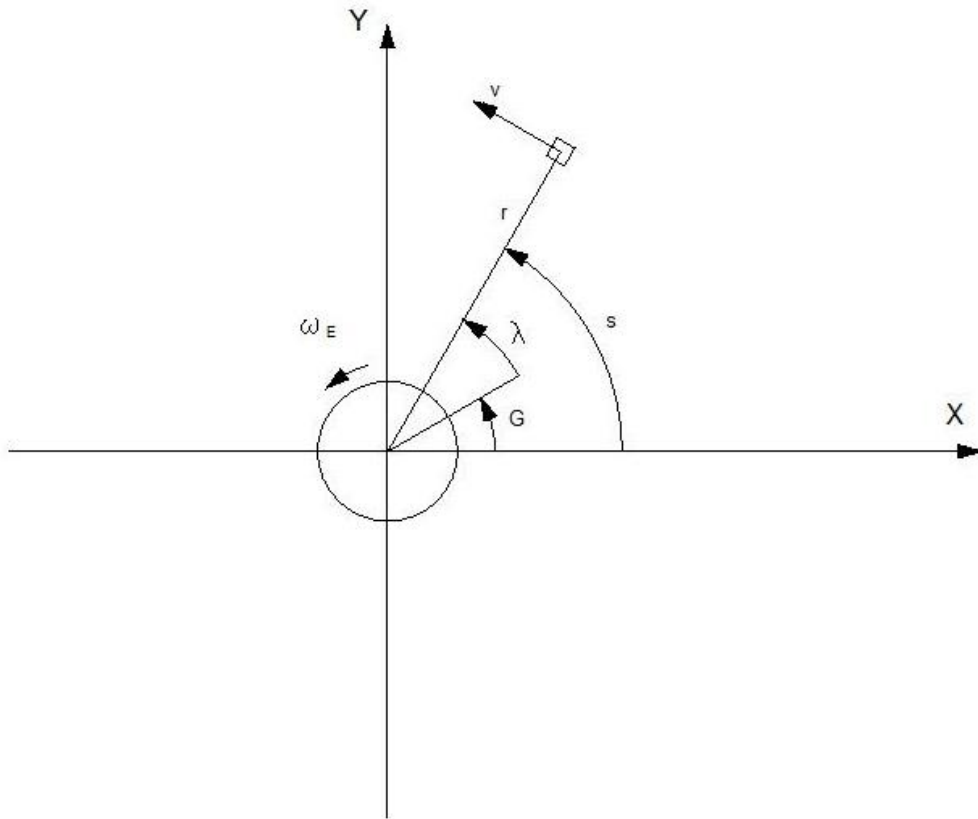
Figure 1: The MEGSD Coordinate System [1].

The three reference frames used throughout this project are depicted in Figure 2.

The ECEF frame, made up of directions I, J, and K, is rotated from the ECI frame by

Greenwich angle G. The spacecraft-oriented coordinate system in Figure 2, known as the

Local-Vertical Local-Horizontal (LVLH) frame, uses the same *I* axis as the ECEF system

– corrected by λ to define the longitude, but is translated out to the radius of the satellite.

Here, ϕ is tangential (east for a satellite in GEO), and the radial (*r*) direction is outward

from the Earth. All three coordinate systems share the same direction for North – with

ECI and ECEF frames utilizing the same axis (seen as *Z, K*), whereas the North axis for

the satellite LVLH frame is translated out to the satellite. The depiction in Figure 2 is the

ideal case for a perfectly geostationary satellite.
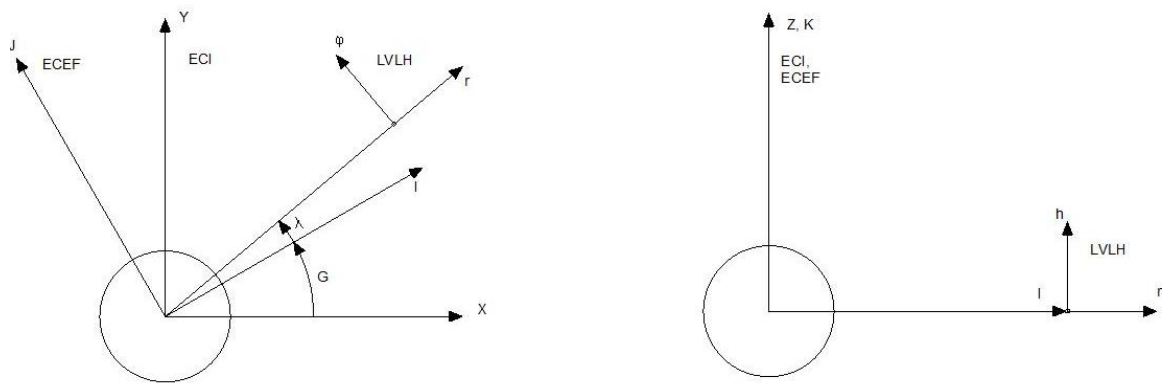
Figure 2: The Earth and Spacecraft Reference Frames.

In April 2010, a cable communications satellite known as Galaxy 15 stopped

receiving inputs to its onboard orbit correction systems. Over a period of nine months,

the satellite gradually drifted until the solar panels pointed away from the Sun long

enough to drain the battery and reset the onboard computers [5]. After the reset, the

satellite once again started receiving inputs from ground control and was able to correct

its orbit and attitude to resume use as a cable satellite. This failure and restart, not

incomparable to rebooting a problem computer, is why Galaxy 15 is considered a

"zombie" satellite. Galaxy 15 is a verified occurrence of a zombie satellite, a term

reserved for satellites that have drifted or ended their missions, and then reinstated at a

later date [6]. During its zombie state, Galaxy 15 was not under the control of ground stations; in fact, the satellite simply drifted. The satellite trajectory was dictated by astrodynamic forces alone, including solar, lunar, and Earth's gravitation forces, instead of ground control.

The final point of interest in this particular satellite comes from its onboard Wide Angle Augmentation System (WAAS). To improve the positioning information of satellites, the U.S. Military has been working on the WAAS since 1994 [7]. This system measures GPS coordinates between multiple satellites and their locations against each other, and corrects these coordinates by finding and eliminating errors [7]. This positioning system is implemented on Galaxy 15, and was transmitting position data from the satellite as it drifted unresponsive to ground control. While the onboard controls were unresponsive, the WAAS continued to output the satellite's position and velocity ephemerides as it drifted around the Earth. Using up the battery as the satellite lost power, the data transmission stopped for a period of about five weeks, but the rest of the drift data can be used to model and determine the significant forces on a satellite as it is free from ground control corrections. These drift data can then be compared to models featuring the theoretical perturbations from all the considered forces that act on a satellite. As a majority of the satellite-specific forces are small, with solar pressure being the only considered force concerned about the spacecraft shape [1], this analysis can be applied to other satellites in the same orbit regime with similar attitude characteristics, or modified to account for attitude differences.

Review of Literature

Geosynchronous Force Models

Models concerning the operative forces at or near GEO come from extending analyses from other observations. The Newtonian point-mass gravitational forces are calculated based on the known distances and masses from the original gravitational equations. However, the elliptic nature of Earth's gravitational field must be accounted for [8], and the non-spherical harmonics are so powerful they need to be modeled at least to the eighth degree. Additionally, solar pressure has been found to have a large effect on satellites [9], and solar wind *could* have an effect during a geomagnetic storm [10], but is negligible in normal conditions [1]. However, it has also been shown that only the major gravitational forces really have an effect on perturbations [11] – for instance, a satellite in GEO is barely affected by Jupiter's moon Ganymede. Studies looking at uncontrolled objects in GEO often use these baseline concepts, such as the investigation by Aslanov *et al.* [12].

Geosynchronous Satellite Modeling

Plenty of models exist for modeling satellites in orbit, and the geosynchronous orbit is a dynamically complex and highly-populated orbit, meaning many studies have already been generated for this particular orbit. A simple classroom model, which demonstrates the fundamental characteristics, is used to teach the basics of geostationary orbit, and is immediately available online [13]. More complex models are generally for specific operational purposes, and others can be found for simple instructional purposes. Other, far more precise models, are used in the orbit estimation and correction of the

actual satellites [14]. While the simpler models are easy to obtain, they do not feature the accuracy required for this capstone project. The most complex models are not readily acquired, and thus are not practical for this purpose. Thus, in the fulfillment of this work a high-fidelity model has been generated. None of these previous models have been used to publish information on the drift portion of Galaxy 15's lifetime.

Galaxy 15

Articles contemporary with the event show that control of Galaxy 15 was lost as a result of an energetic particle injection and acceleration during a magnetic storm [15]. Additionally, the recovery of the satellite was managed after the batteries were drained and the satellite was rebooted, when the operators began to slowly retake control of the satellite [16]. Few articles exist showing the actual path the satellite took, aside from articles that describe the concern that there would be data transmission disruption between Galaxy 15 and AMC 11, or that the customers serviced by Galaxy 15 were switched to Galaxy 12 until control was regained of the rogue satellite [17]. Finally, Shallberg, Potter, and Class indicate that Galaxy 15 "orbited from its assigned orbital location of 133W to 97W" over the nine-month period in their article concerning WAAS refinement [18].

PROJECT DESCRIPTION

In this project, a simple point-mass spacecraft was modeled, and put into a dynamic system focusing on geosynchronous orbit about the Earth's gravity field. Using a point approximation for the acceleration on the satellite due to Earth's gravity, a relatively simple orbit path can be generated. This original orbit is the perturbation-free model that the satellite *would* follow if the Earth was truly a point mass and no other perturbations existed. Data from the satellite already show it is not this simple: further perturbation movements, including the Moon's gravity field, the Sun's gravity field, and solar pressure, were then added to the model. The accelerations from these forces, specifically, were used to model the acceleration of the satellite. The trajectory was then integrated out of the acceleration by finding the position and velocity for a finite number of points. Finally, this orbit was compared with the actual drift orbit of Galaxy 15, accurate to about 1 meter per axis, to quantify whether the drift differs greatly from the theoretical model. Galaxy 15 ephemerides consist of actual position and velocity data, so a comparison at this point was feasible, but as the satellite inevitably drifts in multiple dimensions, the comparison was still not a simple task. The modeling in this project was done in the mathematical matrix laboratory Matlab ®, as it is ideal for large iterations of differential equations – such as those necessary to track the orbits and gravity fields of a satellite. Matlab ®'s interior program, ODE45 (Ordinary Differential Equation solver based on the Runge-Kutta 4,5 method), was also heavily utilized in this project to perform the numerical integrations necessary to find the velocity and position changes from the acceleration.

Justification

Humans have been launching satellites into orbit around the Earth since Sputnik in 1957. That is over a half century of time in space, and in this half century, thousands of different satellites, probes, and other spacecraft have been sent out into space [19].

To date, over 450 satellites have been launched into geostationary orbit [20], as displayed in Figure 3. These satellites range from military, to commercial, to governmental projects, and they all need orbit corrections throughout their mission durations. This specific orbit, GEO, has actually grown crowded over the past few decades, and satellites at the ends of their missions have had to reserve fuel to move to 'graveyards' outside of geosynchronous orbit [1]. Additionally, this is perhaps the conceptually simplest orbit area to study, as ideally the spacecraft's longitude is constant, and the latitude should always be near 0°, or along the equator. As this particular satellite – Galaxy 15 – is the only satellite to drift freely for months while sending out precision position data, its orbit is the only one that can be studied in this way.
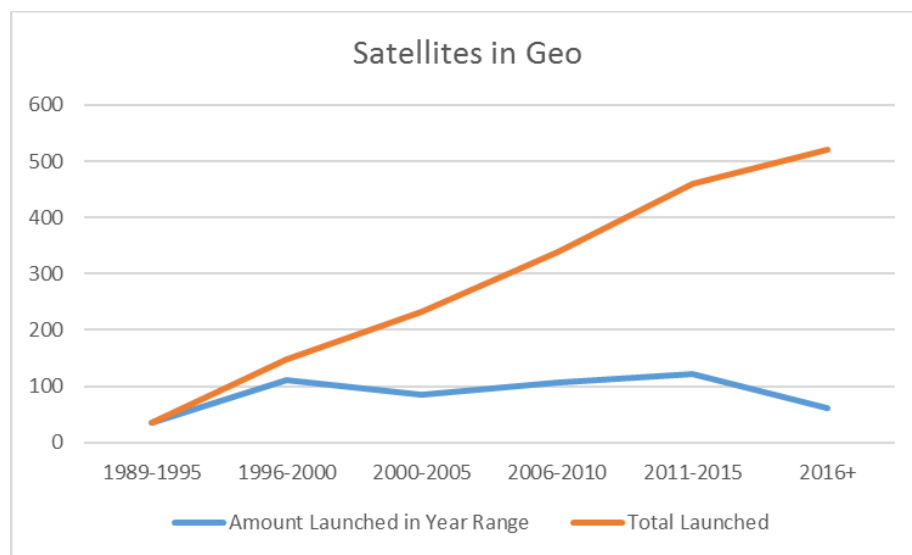
Figure 3: Satellites Launched into Geostationary Orbit [20].

Orbital Dynamics

Many satellites pointed towards Earth follow a geosynchronous orbit. This orbit is at the radius necessary to orbit the Earth at the same speed the Earth revolves, and is in the equatorial plane, so the satellite is really above the same portion of Earth at all times. This is just a simplification, as perturbative forces will cause the satellites to drift around their designated locations; however, it is a good starting point.

Soop [1] presents that, taken as a point mass, the force due to the gravitation field around Earth follows from Newton's laws as

$$\vec{F} = -\frac{m\mu}{r^3}\vec{r} \ . \tag{1}$$

In order to maintain a circular orbit, the velocity must determine the radius, or the radius determines the velocity. Thus, for a relative angular velocity of zero with the Earth – to provide for geosynchronous orbit – the radius r is dependent on the gravitational constant μ. Thus, this equation can be solved [1] to find the ideal radius, A, for the velocity to be one revolution per day per:

$$A = \sqrt[3]{\frac{\mu}{\omega_E{}^2}} = 42164.2 \ km. \tag{2}$$

This distance is measured from the point-mass assumed as the center of the Earth and the center of its gravity. Any satellite operating in GEO will have a mean radius of A; however, eccentric orbits are common, and the actual radius for a satellite is rarely actually the value calculated in Equation (2) [1].

In a three-dimensional world, position is given at three dimensions. With the radius, or the distance to the center of the Earth already given, one is eliminated. Next, in order to be truly geostationary, the satellite must lie along the same plane as Earth's equator, or the *Equatorial Plane*. Thus, two of the three dimensions are given. The final

dimension is the longitude, or at which angular location around the Earth the satellite will remain. This dimension is the only dimension of freedom the satellite operator actually has when considering position.

With three-dimensional positions come three-dimensional velocities. In the standard coordinate system for the satellite, tangential (forward), radial (outward), and orthogonal (North), the velocity equations [1], relative to a *rotating* Earth, become

$$V_t = V(D + 2e_x \cos s + 2e_y \sin s), \tag{3}$$

$$V_r = V(e_x \sin s - e_y \cos s),$$

and
$$V_o = V(i_x \sin s - i_y \cos s).$$

Here, $\bar{e}$ is the eccentricity vector, and $\bar{\iota}$ is the inclination vector. To change to the inertial system, the rotational velocity at the ideal geosynchronous position must be added to the tangential velocity to account for the rotating reference frame. Translation into MEGSD is just a rotation around the north (orthogonal, or *z*) axis by -s, adding the sidereal component in.

Using the vectors presented in Equation (3) gives a complex image of what is happening to the satellite, and is not easy to visualize. Instead, the position and velocity data are used to calculate the Classical Orbital Elements (COE), with Equations (4) through (19).

The complex nature of the forces acting on the satellite necessitate the utilization of multiple reference frames to accurately depict the acceleration of the spacecraft. Rotations between the ECEF and the ECI frames are generally found through the rotation in Equation (4) [21]:

$$\vec{r}_{GCRF} = [P(t)][N(t)][R(t)][W(t)]\vec{r}_{ITRF}. \tag{4}$$

Here, $\vec{r}_{GCRF}$ is the vector to the object of interest in the inertial Geocentric reference

frame, $\vec{r}_{ITRF}$ is the vector in the International Terrestrial reference frame, $\boldsymbol{P}$ is the

precession matrix, $\boldsymbol{N}$ is the nutation matrix, $\boldsymbol{R}$ is the sidereal-rotation matrix, and $\boldsymbol{W}$ is the

polar motion matrix. As this study is on a geosynchronous orbit, precession, nutation,

and polar motion will be neglected. The rotation matrix used in this study and shown in

Equation (5) represents just the sidereal rotation:

$$\vec{r}_{eci} = \begin{bmatrix} \cos(G) & -\sin(G) & 0 \\ \sin(G) & \cos(G) & 0 \\ 0 & 0 & 1 \end{bmatrix} \vec{r}_{ecef} . \tag{5}$$

Additional translations are necessary to go into the satellite Local Vertical Local

Horizontal (LVLH) frame, also known as the Satellite Coordinate System. This is the

most straightforward coordinate system to model the accelerations on the spacecraft. In

this project, accelerations are determined in their more convenient reference frames, and

then translated and rotated into the LVLH frame for determination of how the forces

affect the satellite. For this translation, from ECI to LVLH, three unit vectors are created

from the inertial position and velocity data of the satellite, per Equation (6) [21]:

$$\vec{r}_{eci} = \left[\frac{\vec{r}}{|\vec{r}|}, \frac{\vec{r} \times \vec{v}}{|\vec{r} \times \vec{v}|} \times \frac{\vec{r}}{|\vec{r}|}, \frac{\vec{r} \times \vec{v}}{|\vec{r} \times \vec{v}|} \right] \vec{r}_{LVLH}. \tag{6}$$

However, using the position and velocity information is not very conducive to visualizing

the actual orbit propagation. Instead, the COE's, such as longitude and inclination, will

be utilized to properly understand how the satellite moved. To generate the COE, the

position and velocity vectors must first be defined, from Equations (7) and (8) [21]:

$$\vec{r} = x\hat{\imath}_x + y\hat{\imath}_y + z\hat{\imath}_z \tag{7}$$

and

$$\vec{V} = dx\hat{\imath}_x + dy\hat{\imath}_y + dz\hat{\imath}_z. \tag{8}$$

Next, the angular momentum vector can be found by crossing the position and velocity, as Equation (9) shows:

$$\vec{h} = \vec{r} \times \vec{V}.$$ (9)

From this equation, the vector pointing to the ascending node is found through Equation (10):

$$\vec{n} = \hat{\imath}_z \times \vec{h}.$$ (10)

Now, from these variables, the eccentricity vector can be found through the complicated Equation (11):

$$\vec{e} = \frac{\left(V^2 - \frac{\mu}{r}\right)\vec{r} - (\vec{r} \cdot \vec{V})\vec{r}}{\mu}.$$ (11)

The eccentricity found in Equation (11) is one of the major identifying elements for the orbit, and this vector is used to represent how the orbit of Galaxy 15 changed. Another important element, the Semi-Major Axis, can be found through the use of specific mechanical energy, which is given in Equation (12):

$$\xi = \frac{V^2}{2} - \frac{\mu}{r}.$$ (12)

Now, the semi-major axis is found through Equation (13):

$$a = - \frac{\mu}{2\xi}.$$ (13)

This can then be normalized to the semi-major axis offset from nominal by means of Equation (14) [21]:

$$\Delta \bar{a} = \frac{a - A}{A}.$$ (14)

Other important orbital elements include the inclination, found through Equation (15), the right ascension of the ascending node from Equation (16), the argument of

perigee from Equation (17), the true anomaly through Equation (18), and finally, the

longitude through Equation (19):

$$\vec{\iota} = \cos^{-1}\frac{\hat{\iota}_z \cdot \vec{h}}{|\hat{\iota}_z||\vec{h}|}, \tag{15}$$

$$\Omega = \cos^{-1}\frac{\widehat{\iota_y} \cdot \vec{n}}{|\vec{n}|}, \tag{16}$$

$$\omega = \cos^{-1}\frac{\vec{n} \cdot \vec{e}}{|\vec{n}||\vec{e}|}, \tag{17}$$

$$\upsilon = \cos^{-1}\frac{\vec{e} \cdot \vec{r}}{|\vec{e}||\vec{r}|}, \tag{18}$$

and

$$\lambda = \cos^{-1}\frac{\hat{\iota}_y \cdot \vec{r}}{|\vec{r}|}. \tag{19}$$

Satellite Perturbations

Until now, the only force on the satellite considered is due to Earth's point mass

gravity. As indicated before, this is a simplification. The Sun also has a realizable

gravitation pull, as does the Moon, and even the ellipsoidal non-homogeneous nature of

the Earth! The Sun also emits solar radiation pressure on the effective Sun-oriented

surface area of the craft. As the craft changes orientation, the effective surface area will

change. Additionally, Earth is tilted to the ecliptic plane, so the equator does not line up

with the ecliptic, meaning the Sun will also have a slight northward and southward pull

on the satellite each year, and the Moon is even further out-of-plane, and also provides an

acceleration based on its orbit. Figure 4 displays a very simplified image of the relevant

perturbative forces acting on a satellite.
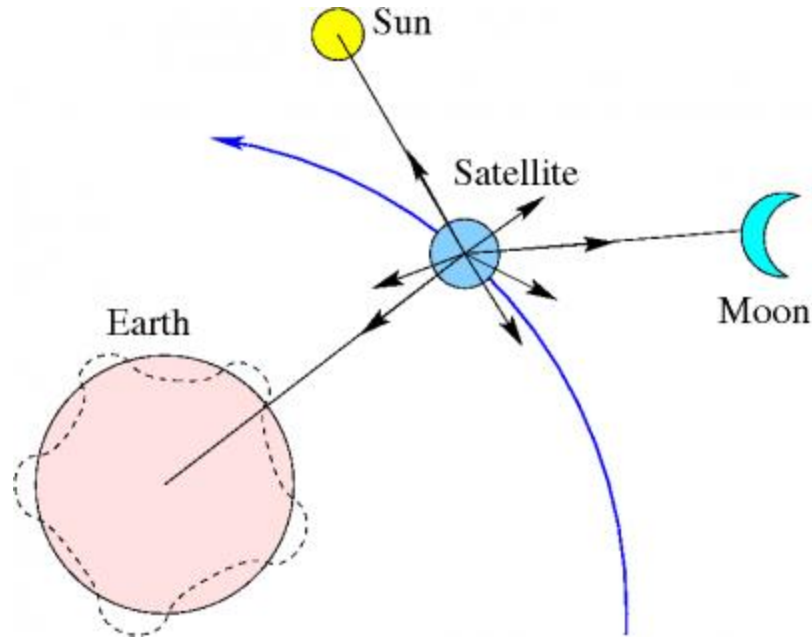
Figure 4: Satellite Gravitational Perturbation Forces [22].

In actuality, each and every celestial body has a gravitational impact on every other celestial body [23]. However, down to a point, this impact becomes negligible. For instance, of all celestial bodies outside the Earth, Sun, and Moon, Venus has the largest gravitational impact on satellites in Earth's geosynchronous orbit, but even Venus' effect is so small it is considered negligible for a full year's orbit – Venus' pull is, at a maximum, five orders of magnitude smaller than the Sun's [1]. Several other forces of even smaller magnitude are also neglected, as they have a relatively tiny impact on the station-keeping of a satellite. However, these small gravitational forces move the satellite outside of its ideal position.

Each of the perturbing forces provide an acceleration on the satellite. These accelerations can all be added together to find the full acceleration of the satellite at any point in time. These accelerations are then implemented into the satellite's accelerations with the series of Equations (20) through (25) given by Tombasco [24]:

$$\dot{\lambda} = \frac{h}{r^2} + \frac{r}{h}\tan\left(\frac{i}{2}\right)\sin(w+v)\,a_h - \omega_e, \tag{20}$$

$$\Delta\dot{a} = \frac{2A(\Delta\bar{a}+1)^2}{h}\left[\left(e_x\sin(s) - e_y\cos(s)\right)a_r + \frac{p}{r}a_\phi\right], \tag{21}$$

$$\dot{e}_x = \frac{r}{h}\left\{\frac{p}{r}\sin(s)\,a_r + \left[e_x + \left(1+\frac{p}{r}\right)\cos(s)\right]a_\phi\right\} + e_y\frac{r}{h}\left\{\left[\tan\left(\frac{i}{2}\right)\sin(\Omega)\cos(s) - \right.\right.$$

$$\left.\left. \tan\left(\frac{i}{2}\right)\sin(s)\cos(\Omega)\right]a_h\right\}, \tag{22}$$

$$\dot{e}_y = \frac{r}{h}\left\{\frac{-p}{r}\cos(s)\,a_r + \left[e_y + \left(1+\frac{p}{r}\right)\sin(s)\right]a_\phi\right\} - e_x\frac{r}{h}\left\{\left[\tan\left(\frac{i}{2}\right)\sin(\Omega)\cos(s) - \right.\right.$$

$$\left.\left. \tan\left(\frac{i}{2}\right)\sin(s)\cos(\Omega)\right]a_h\right\}, \tag{23}$$

$$\dot{i}_x = \left[\frac{r}{h}\sin(\Omega)\cos(\omega+v) + \frac{ir}{h\sin(i)}\cos(\Omega)\sin(\omega+v)\right]a_h, \tag{24}$$

$$\dot{i}_y = \left[\frac{ir}{h\sin(i)}\sin(\Omega)\sin(\omega+v) - \frac{r}{h}\cos(\Omega)\cos(\omega+v)\right]a_h. \tag{25}$$

Here, the acceleration vector $\vec{a} = [a_r, a_\phi, a_h]$.

Gravitation of Earth

  The ellipsoidal non-homogeneous nature of the Earth provides an acceleration

gradient that forces near satellites to accelerate in a different way than if the Earth were a

mere point-mass. In GEO, this gradient provides a slight north or south (the opposite of

whether the satellite is north or south of the equator) acceleration of about 2.95 x 10^{-9}

m/s^2, and a slight inward acceleration of about 8.33 x 10^{-6} m/s^2 [1]. This acceleration

requires a periodic eastward burn to correct, as well as periodic north or southward burns.

These burns result in a parabolic-shaped libration about the mean position, and actually

increase the effective geosynchronous radius by about one-half kilometer [1].

  In order to accurately model the Earth's full gravitational acceleration on the

satellite, the coordinates of the satellite need to be rotated to the ECEF frame from the

ECI frame through Equation (5). From here, a complex set of equations relying on longitude, already calculated in λ, the radius r, and the latitude ϕ, can be calculated from Equation (26):

$$\tan \phi = \frac{r_{ECEF}(3)}{\sqrt{r_{ECEF}(1)^2 + r_{ECEF}(2)^2}}. \tag{26}$$

From here, the non-spherical gravitation about the Earth can be found through the following three derivatives [21]:

$$\frac{\partial U}{\partial r} = -\frac{\mu}{r^2} \sum_{l=2}^{\infty} \sum_{m=0}^{l} \left(\frac{R}{r}\right)^l (l+1) \, P_{l,m}[\sin\phi]\left(C_{l,m}\cos(m\lambda) + S_{l,m}\sin(m\lambda)\right), \tag{27}$$

$$\frac{\partial U}{\partial \phi} = \frac{\mu}{r} \sum_{l=2}^{\infty} \sum_{m=0}^{l} \left(\frac{R}{r}\right)^l \left(P_{l,m+1}[\sin\phi] - m\tan\phi \, P_{l,m}[\sin\phi]\right)\left(C_{l,m}\cos(m\lambda) +$$

$$S_{l,m}\sin(m\lambda)\right), \tag{28}$$

and $\quad \frac{\partial U}{\partial \lambda} = \frac{\mu}{r} \sum_{l=2}^{\infty} \sum_{m=0}^{l} \left(\frac{R}{r}\right)^l m P_{l,m}[\sin\phi]\left(S_{l,m}\cos(m\lambda) - C_{l,m}\sin(m\lambda)\right). \tag{29}$

These equations utilize the mean equatorial radius of Earth, R, the distance from Earth to the satellite, r, the computed gravitational harmonic components S and C, found online at the NASA and German Space Agency (DLR) GRACE website presented by the University of Texas [25], and the Legendre polynomials P as a function of the sine of ϕ, as presented in Appendix A – normalized with Equations (30) and (31):

$$\Pi_{l,m} = \sqrt{\frac{(l+m)!}{(l-m)!k(2l+1)}} \tag{30}$$

and $$\bar{P}_{l,m} = \frac{P_{l,m}}{\Pi_{l,m}}. \tag{31}$$

The further out the first sum is taken, the more accurate the model will be. In reality, however, for GEO objects, the model only needs to go out to 8 or so sums to have an accurate model of the orbit path, and in this study, the summation was capped at 8 sums. Once these derivatives are found, they can be combined into the accelerations in the

satellite reference frame, I, J, and K directions within the ECEF frame, using Equations (32) through (34) [21]:

$$a_I = \left(\frac{1}{r}\frac{\partial U}{\partial r} - \frac{r_K}{r^2\sqrt{r_I^2+r_J^2}}\frac{\partial U}{\partial \phi}\right)r_I - \left(\frac{1}{r_I^2+r_J^2}\frac{\partial U}{\partial \lambda}\right)r_J, \tag{32}$$

$$a_J = \left(\frac{1}{r}\frac{\partial U}{\partial r} - \frac{r_K}{r^2\sqrt{r_I^2+r_J^2}}\frac{\partial U}{\partial \phi}\right)r_J + \left(\frac{1}{r_I^2+r_J^2}\frac{\partial U}{\partial \lambda}\right)r_I, \tag{33}$$

and
$$a_K = \frac{1}{r}\frac{\partial U}{\partial r}r_K + \frac{\sqrt{r_I^2+r_J^2}}{r^2}\frac{\partial U}{\partial \phi}. \tag{34}$$

Once the accelerations are found in the ECEF frame, they need to be rotated back to the ECI frame by Equation (5) for the combination of the other perturbation accelerations.

Solar and Lunar Gravity

The Sun and Moon provide for similar, yet complexly linked, gravitational effects on the satellite. As the distances between the satellite and Sun and the satellite and Moon are not constant, they provide sinusoidal accelerations. As they are both sinusoidal, over a long enough time-span, their respective effects nearly average out [1]. Another sinusoidal effect arises from the fact that the satellite will orbit on a plane inclined to the ecliptic plane. This means that in addition to the effects that the Sun and Moon have on the satellite's tangential motion, they will also cause the inclination vector to drift, as displayed in Figure 5. Problems arise when the accelerations cause the satellites to drift far enough off course that they can no longer function properly, or need to be re-adjusted so as not to collide with any other orbiting bodies. Using Equation (35), the gravitational

acceleration on the satellite from these sources can be found [1], employing the

ephemerides published by the Jet Propulsion Laboratory (JPL):

$$\frac{d^2\bar{r}}{dt^2} = -\frac{\mu}{r^3}\bar{r} + \sum_{k=1}^{2}\mu_k\left[\frac{\overline{r_k}-\bar{r}}{|\overline{r_k}-\bar{r}|^3} - \frac{\overline{r_k}}{r_k^3}\right]. \tag{35}$$

Here, no subscript indicates Earth, a subscript of 1 indicates the Moon, and a subscript of

2 indicates the Sun. As this equation takes into account the gravitational pull of Earth

alone, which has already been considered, the first term (before the summation) in

Equation (35) should be replaced with zero (0). As the ephemerides provided are given

once per day, a polynomial was fit to these ephemerides and the position vectors to the
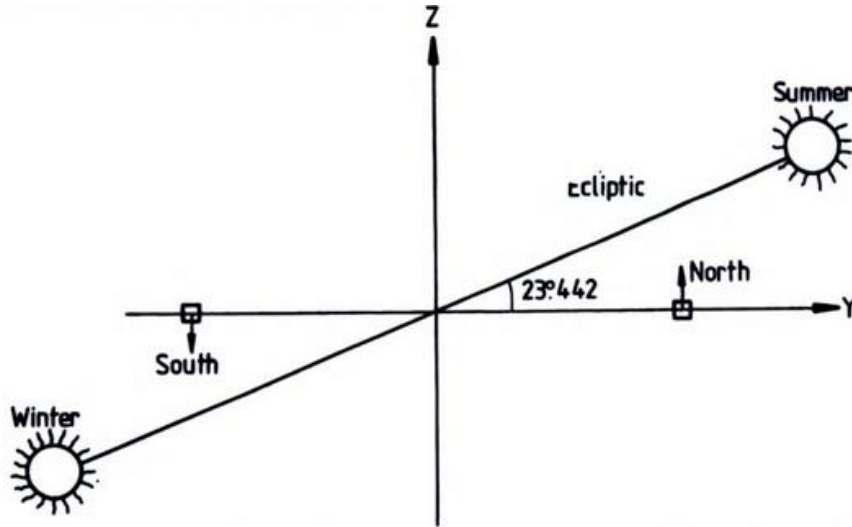
Sun and Moon were extrapolated for the full data.

Figure 5: Torque Applied to Inclination Vector by the Sun [1].

The Moon's orbit itself does not lie on the ecliptic, so it also experiences the same

inclination drift from the Sun. However, as the Sun will provide a positive acceleration

northward for half of the year, and a negative acceleration northward for half of the year,

the actual north-south drift averages out. Yet, a torque is applied to the satellite, forcing

the actual inclination vector of the satellite to drift. This drift gently pulls the satellite off

of the equator. For a short mission, this effect can generally be neglected, but these small

torques need to be considered over a multi-year mission.

Solar Radiation Pressure

Potentially the most complex to model, and the smallest non-negligible effect

traditionally considered, solar radiation pressure comes from solar activity of the Sun [1].

This radiation emits a mean pressure on everything facing it, thus putting a relatively

constant force on the solar panels of the satellite. Solar radiation only has a real effect on

the eccentricity of the orbit, as the mean effect over a day should cancel in all other

directions. The acceleration due to the solar radiation pressure comes from Equation (36)

[21]:

$$\vec{a}_{sr} = -\frac{p_{sr} c_R A_s}{m} \frac{\vec{r}}{|\vec{r}|}.$$
(36)

In Equation (36), p_{sr} is the pressure from the Sun, estimated here at 4.56×10^{-6} N/m^2 [21],

c_R is the reflectivity of the surface facing the sun ranging from 0 to 2, and A_s is the

surface area of the satellite. In this study, the reflectivity is assumed to be 1.35, a value

similar to most solar panels [26]. The surface area is the most complex part of this

equation. In reality, the satellite slowly tumbled – however, the reaction wheels on board

should have been keeping the satellite's attitude mostly pointed at the Sun, but the only

way to verify this is to either obtain attitude data or examine power data from Galaxy 15

as it drifted. An assumed value of 20 m^2 is used here, similar to most GEO

communication satellites [27].

METHODS

This project was completed in three phases. The first phase centered on assessing the behavior experienced by Galaxy 15 as it drifted in the first month after control was lost. The second phase focused on a force model construction at GEO, including several perturbation forces, and placed a model satellite in the force model to examine the behavior. The final phase then entailed taking the actual trajectory from the first phase and comparing it to the predicted trajectory from the second phase. From here, potential conclusions can be formed based on the differences noted, such as the direction of the difference between the two paths, indicating which force had the largest non-modeled effect, or whether the model was sufficient to examine all forces the satellite was subjected to.

Orbital Evolution of Galaxy 15

The first phase of the project entailed the investigation of the actual trajectory carried out by Galaxy 15 in the first month after control was lost. This trajectory was compared to the trajectory followed for a similar timespan and orbit when the satellite was under full control to clarify the full drift the satellite experienced. This alone can give great insight into the orbital effects on the satellite, and can lead to conclusions about the relative forces causing the perturbations on the satellite itself.

Force Model for Geosynchronous Orbit

The second project phase, focusing on the force model at GEO, began with construction of the model. The force model starts with a simple dynamic system of the

Earth and Galaxy 15 in an idealized point mass GEO orbit. From here, the perturbation effects outlined in the background were added in one by one, and the results verified against the actual trajectory of the satellite. The last perturbation force, the solar pressure, needed to be simplified for this study. Instead of using the actual spacecraft shape and attitude to determine the effective surface area to mass ratio needed for the calculation, a constant estimation was used – recognized as a 'cannonball' model. This was necessitated by the lack of publicly available attitude data, and was achieved by assuming a spherical satellite shape, and using the circular surface area aimed towards the Sun as the surface for the pressure to act against. This assumption is not accurate over the nearly 10-month period control was lost on the satellite, as eventually power was lost when the solar panels drifted out of orientation with the Sun. However, for the first month, the tumble of the satellite attitude should have been low enough that the assumption is fairly accurate. Additionally, the solar pressure present was assumed constant over this time period, as it would greatly simplify the problem, and would not diverge too much from reality.

These models were constructed in Matlab ® by utilizing the accelerations imparted on the satellite, and the relevant integrations were processed through the onboard ODE45 integration tool. Results were plotted in Matlab ®, as well, and analyses were created from these models. Instead of using a single thirty-day sequence, this model utilized six sets of five days, taking the last data point used in each day as the first in the next in order to fully propagate the model. This was done as computer memory constraints were noted while attempting to run as one solid month.

Trajectory Comparison

The final phase of the project investigated the two trajectories found in the previous two phases, comparing them against each other. As there are several underlying assumptions, it was not expected that the model would perfectly predict the drift of the satellite. In fact, it was recognized that the solar pressure assumptions given in the force model description would likely cause some level of inaccuracy. However, it was clear that the directions and magnitudes of the inaccuracies would show a significant amount of information. If the magnitude of the difference is relatively small, this could mean the assumptions used were fairly accurate, and if they are large, then the assumptions are clearly inaccurate. If the solar pressure assumptions are inaccurate, for instance, the difference between the actual and the expected eccentricity vector drifts should be relatively large. Differences in other directions could also point to other conclusions about other forces.

RESULTS AND DISCUSSION

This section reviews the data gleaned from a comparison of the Galaxy 15 uncontrolled path from May 2010 against its fully controlled path for the month of May in 2016. These results serve as a baseline – to show how far the satellite moved, and how much from its standard position in the month after control was lost. The control year of 2016 was chosen as it is the closest to 2010, celestially, of the data available. The Earth's position with the Sun was off by roughly 0.5 days, and the Earth's position differed by about 1.7 days, from the 2010 data [28]. Utilizing the WAAS data available online [29], the inertial position and velocity data, in the satellite's x-y-z coordinates, can be extracted, and from here computed into the Earth-centric coordinate system into MEGSD orbital elements coordinates via a series of equations, including Equations (7) through (19) [21]. Please note that in both of these periods, gaps in the data exist, resulting in gaps over the presented timespan.

Uncontrolled Flight Path of Galaxy 15

On April 5th, 2010, control of Galaxy 15 was lost as a result of an ion storm. Looking specifically into the data from May of that year, to avoid any of the transient effects of the storm and the loss of control, the actual drift of the satellite can be analyzed. As previously mentioned, the most important variable for geosynchronous satellites is their longitude. This is what really governs their Earth-relative locations, as the radius, inclination, and eccentricity all are pre-defined. Yet, as control of this satellite was lost, other variables changed, and the changes in these other variables are also examined here.

In the following month, Galaxy 15 drifted from its starting location at 132.7 degrees to 131.2 degrees at the end of May. This 1.5 degree change is enormous, as most satellites in this region stay within 0.2 degrees of their target. Considering the orbital radius of roughly 42,000 kilometers, this is a change in position of about 1,000 kilometers (along the arc). Figure 6 displays the longitudinal change for the two months (May 2010 and May 2016). Figure 6 also shows that in 2010, the longitudinal drift of the satellite accelerated, or that a force pulled it away from the starting position. This longitudinal drift is examined further in the theoretical model.
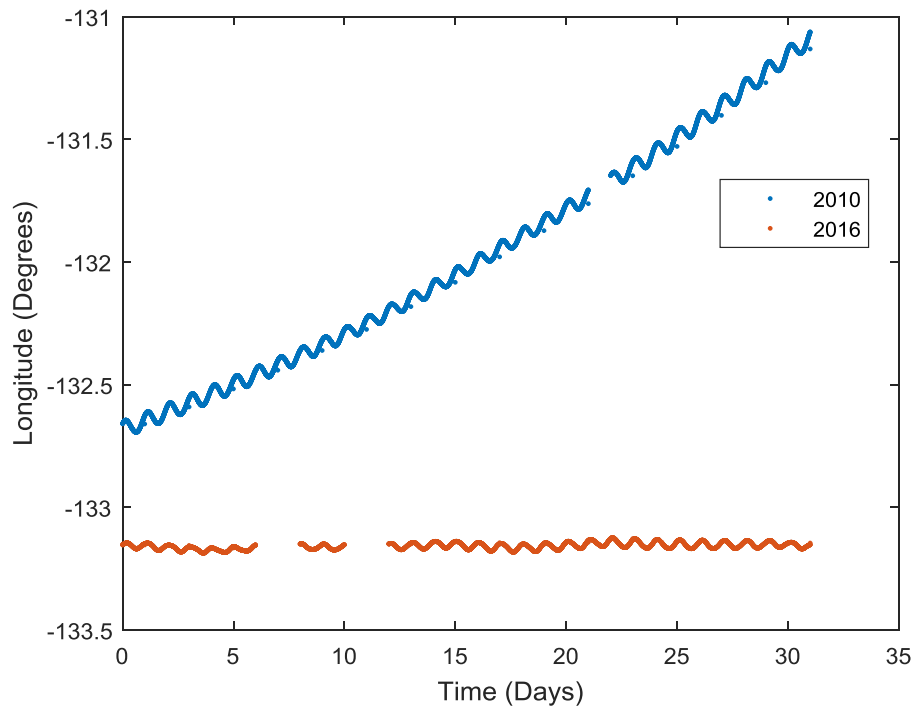
**Figure 6: Galaxy 15 Longitude Drift Comparison, 2010 to 2016.**

The longitudinal drift rate presented in Figure 7 shows the speed at which the longitude of the satellite is changing. It can be clearly seen that the 2016 data have a

relatively constant drift rate, whereas the 2010 data show the drift rate steadily increasing in magnitude – or that the satellite was actually accelerating as it moved from its target longitude. This acceleration can be seen in Figure 6, as the 2010 data do not follow a linear path. The lack of drift for the 2016 data in Figure 6, despite the non-zero drift rate shown in Figure 7, means that the satellite was undergoing orbit corrections at the time, as can be seen more clearly in the satellite's inclination shown in Figure 10.
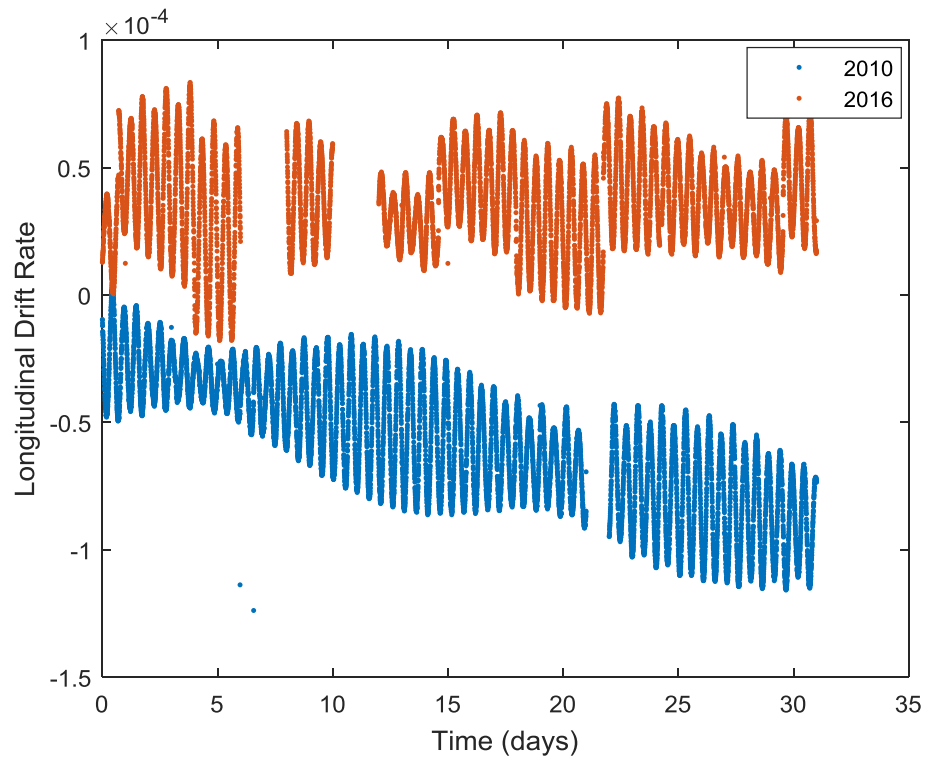

Figure 7: Galaxy 15 Longitudinal Drift Rate ($\Delta\overline{a}$) Comparison, 2010 to 2016.

Figure 8 shows the path the satellite travelled in 2010 and in 2016, as it orbited the Earth. In 2010, the path became more oblong – that is, the periapses became significantly lower, and the apoapses grew slightly. This means the eccentricity of the orbit increased, as Figure 9 shows.
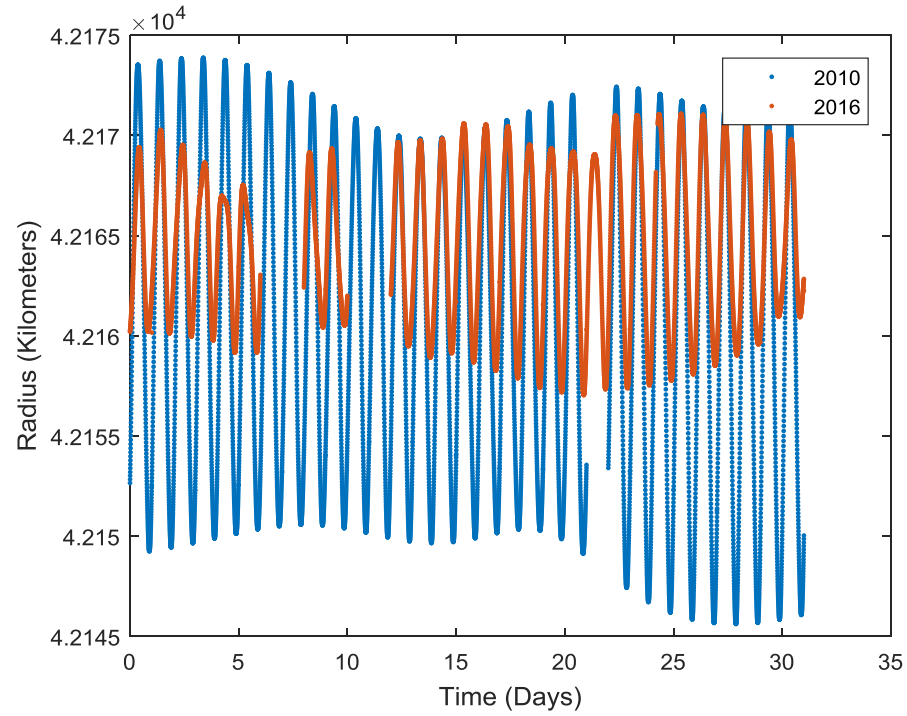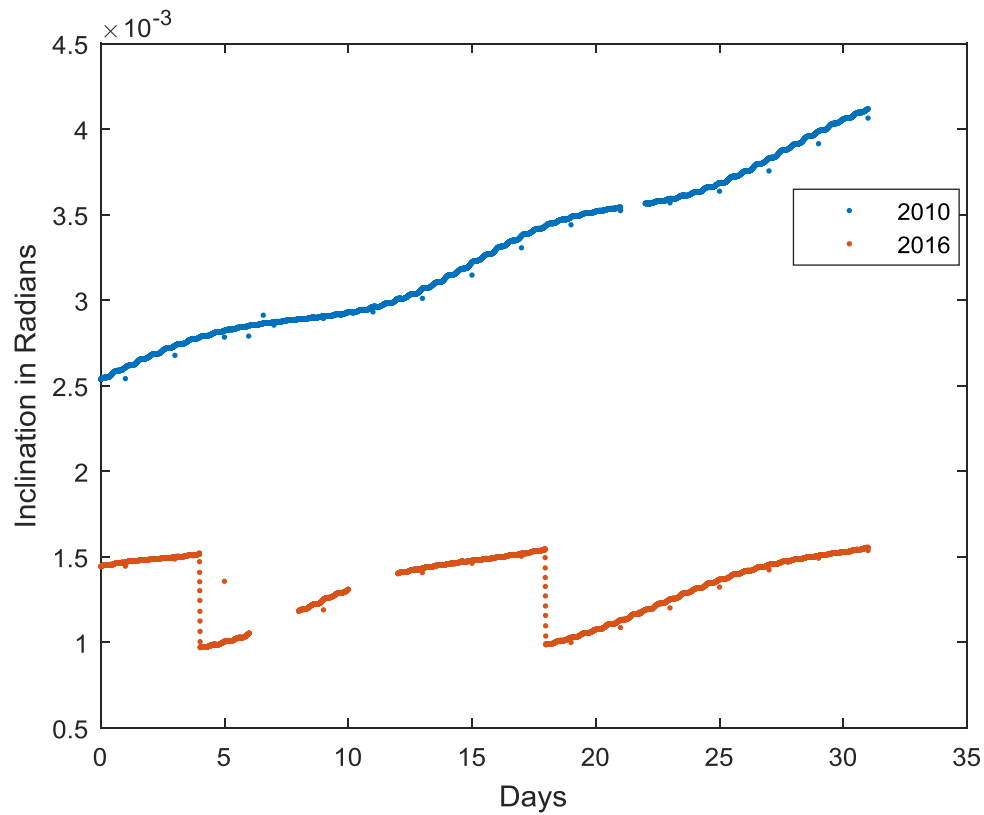
Figure 8: Galaxy 15 Radius Comparison, 2010 to 2016.
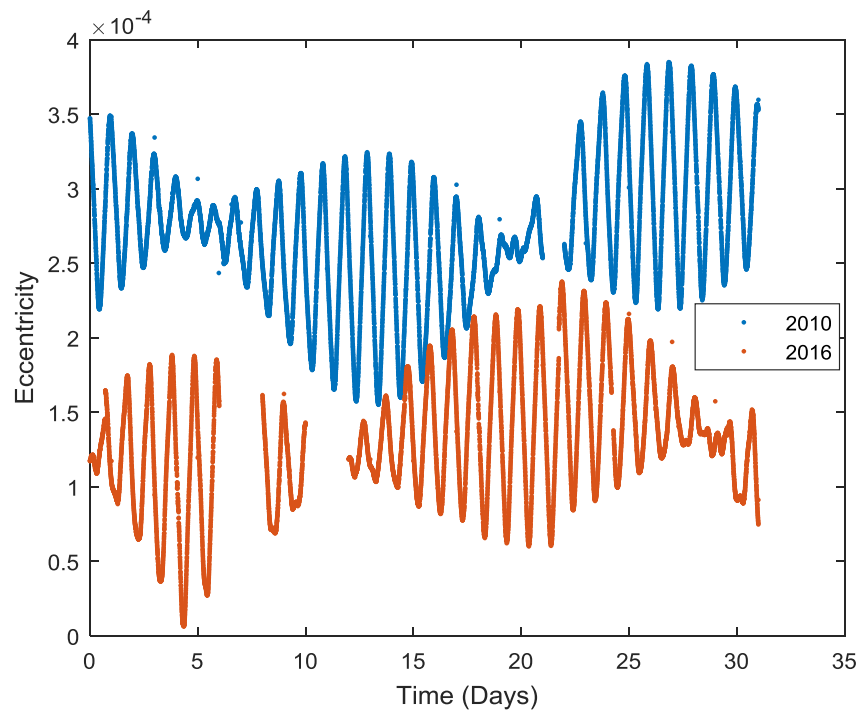
Figure 9: Galaxy 15 Eccentricity Comparison, 2010 to 2016.

Figure 9 displays how the eccentricity of the satellite really increased in 2010.

Though normally the eccentricity is allowed to oscillate, as shown by the 2016 controlled

data, the 2010 increase in the elliptical nature of the orbit indicates that the satellite was

potentially slipping out of its circular orbit.

Finally, the inclinations of the satellite for the months in 2010 and 2016 are

displayed in Figure 10. The results show how the inclination in 2010 continually grew,

in addition to the oscillatory nature. The data from 2016 clearly show movements made

by the control mechanism to correct the drifting inclination.

**Figure 10: Galaxy 15 Inclination Comparison, 2010 to 2016.**

Model Validation

Utilizing Equations (20) through (25), an Ordinary Differential Equation solver,

such as Matlab ®'s ODE45, can be used to propagate over small time-steps over a long

time span, and accurately map the drift of the satellite. This section compares the

modeled drift to the actual drift to validate the model. The structure of the model utilizes

the first data-point of the real 2010 data as a starting point, and then models the satellite

path from there. Mapping the longitudes for thirty days reveals how closely the model is

able to match reality, as Figure 11 shows. As the integration goes longer, the errors start

to accumulate, which is why the real data and the model start to deviate around day 20.
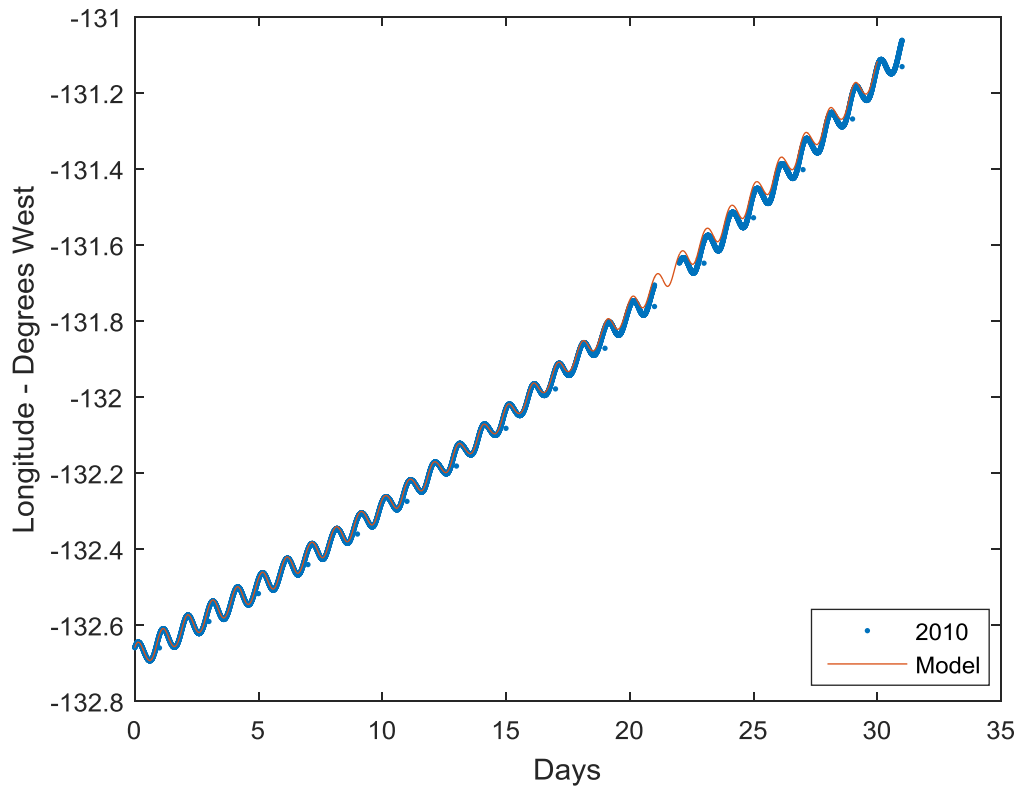
Figure 11: Galaxy 15 Longitude – Real versus Simulated.

Figure 12 displays how closely the modeled longitudinal drift rate follows reality. This has similar results to the longitude – matching very closely initially, but deviating before the final days. Figure 13 shows the differences in the radius. Similar to the other variables, the errors are minimal until the final stretch of the drift.
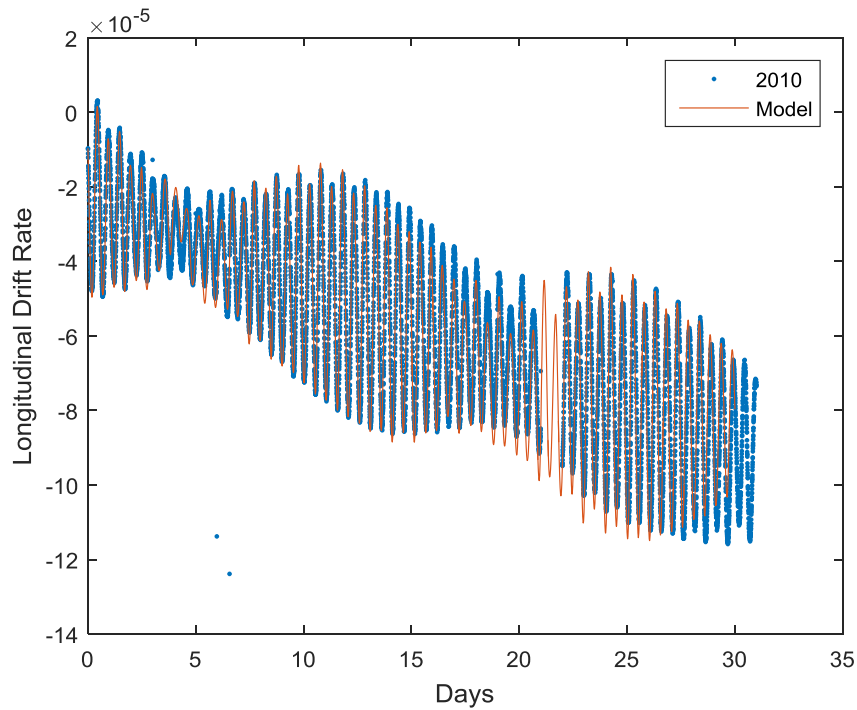
Figure 12: Galaxy 15 $\Delta\bar{a}$ – Real versus Simulated.

On to Figure 14, which shows how closely the eccentricities match between the model and the real data. As stated previously, the larger differences here are likely due to the assumptions on the solar pressure.
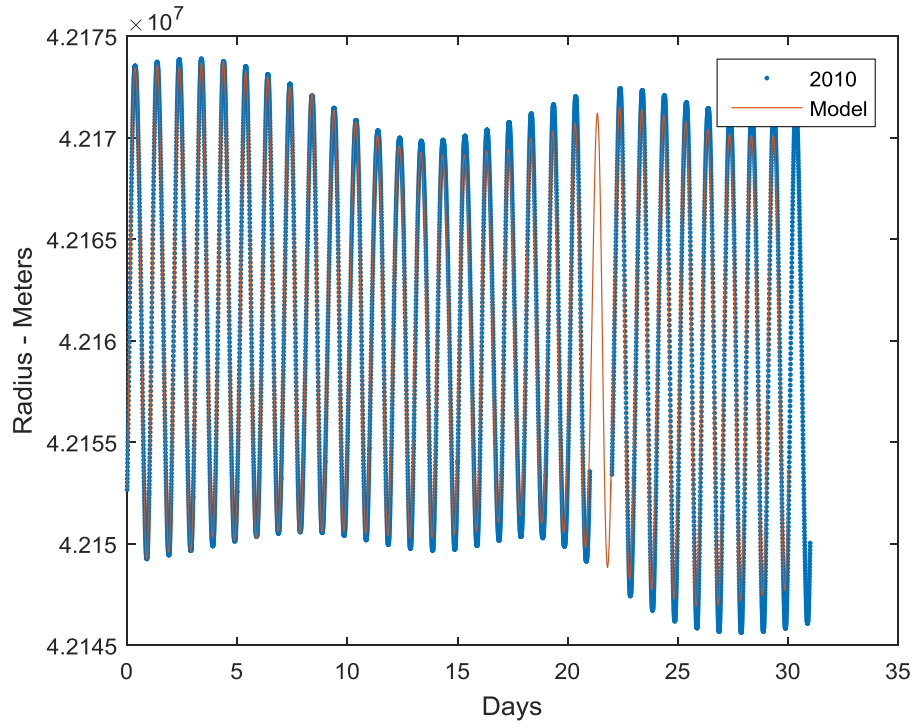
Figure 13: Galaxy 15 Radius – Real versus Simulated.

Figure 14: Galaxy 15 Eccentricity – Real versus Simulated.

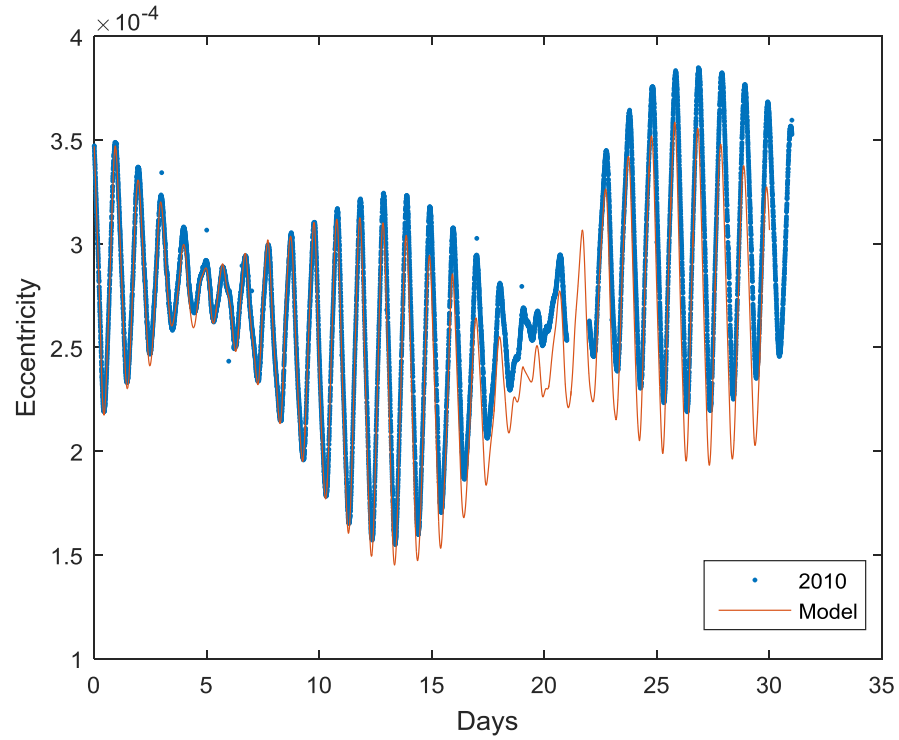Finally, Figure 15 displays how closely the inclination matches between the model and the actual data. Figures 11, 12, 13, 14, and 15 demonstrate that the model is sufficiently valid for the purposes of this project. Thus, with the agreement between the model and the real data, the model can be employed to investigate which perturbation forces cause which COE drifts, as is shown in the following section.
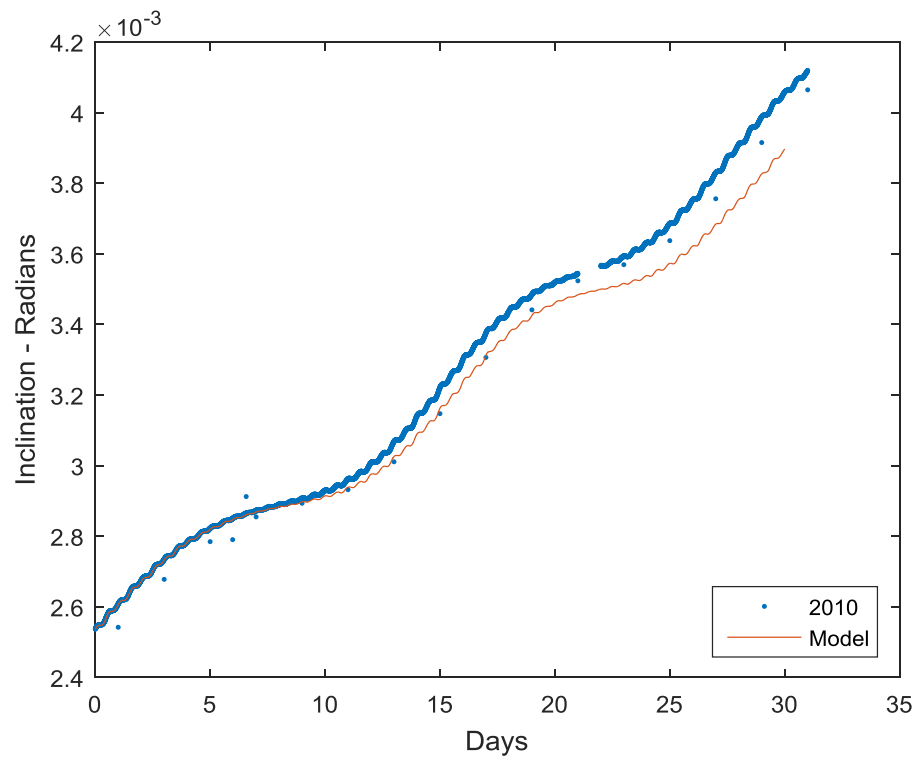
Figure 15: Galaxy 15 Inclination – Real versus Simulated.

Perturbation Force Analysis

Analyzing the model to find each perturbing force's contribution to the orbital path, the results are here shown through visual figures, in a manner similar to the figures employed in the initial analyses. Therefore, in Figures 16 through 25, the legend is interpreted as follows:

Full Model– the full force model utilizing all perturbing forces.

Harmonics – only the non-spherical harmonics of the Earth's gravitation system are considered.

Sun Grav – only the gravitational component of the Sun is considered.

Moon Grav – only the gravitational component of the Moon is considered.

Solar Press – only the perturbing force due to the solar pressure from the sun is considered.

2-Body – only the point-mass model of the Earth gravitational force is considered.

From these contributions, the full model is merely the addition of all the accelerations. Looking first at the longitude, in Figure 16, clearly the simple two-body analysis falls far short of predicting the full flight path.
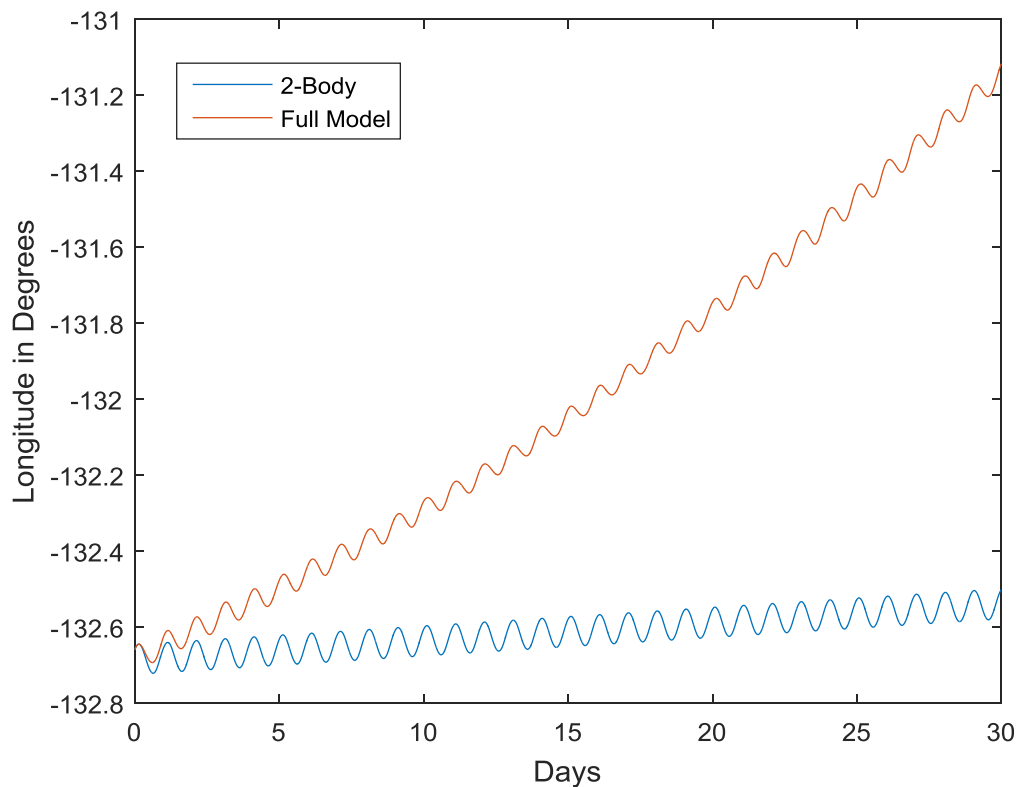
Figure 16: Perturbation Effects on Longitude.

Figure 17 shows how each perturbing force contributes to the difference between the two-body and full model. Clearly, the perturbation from the non-spherical harmonics has the greatest effect on the longitude. Predictably, the solar pressure force had the smallest of the effects on the longitude, barely pushing it slightly westward. The Moon pulled the longitude slightly eastward, and the gravity from the Sun pulled the longitude in the opposite direction that the Moon did, though to a lesser magnitude. Examining Equation (20), it can clearly be seen that the only perturbing acceleration on the satellite longitude is in the satellite northward direction. As the Moon has the greatest actual force in this direction, it seems more likely that the Moon would cause the greater change; however, as the leading term, $\frac{h}{r^2}$, depends on the longitudinal drift rate, which in turn depends on the non-spherical harmonics as shown in the next segment, the non-spherical harmonics are actually the driving force behind the drift in longitude.
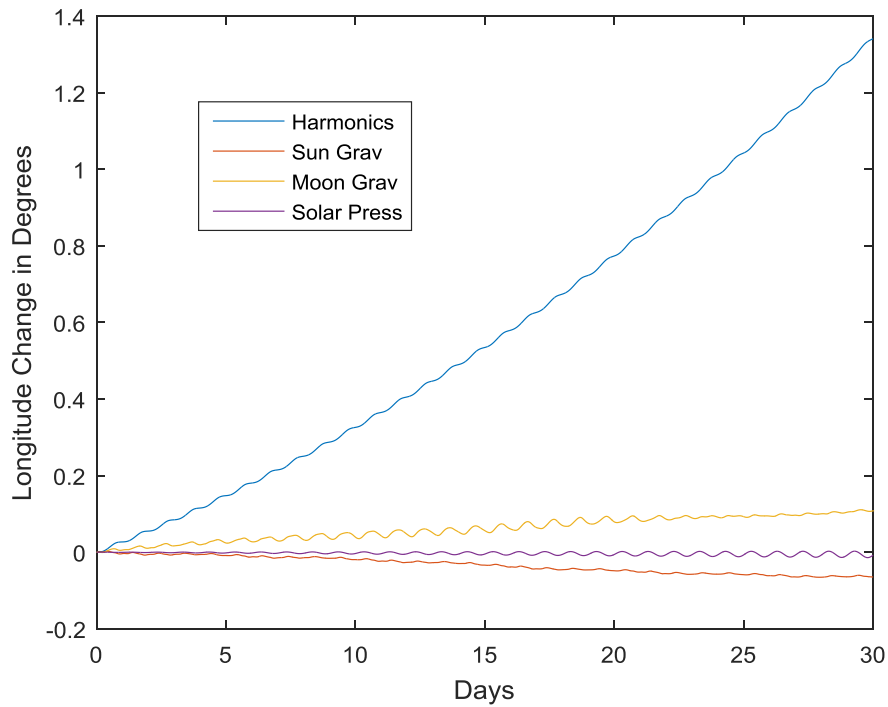
Figure 17: Longitudinal Perturbation Comparison.

The longitudinal drift rate, $\Delta\bar{a}$, shows an extremely complex interaction of forces. Figure 18 indicates that the two-body model predicts none of the path of the longitudinal drift rate – instead all the change comes entirely from the perturbations.
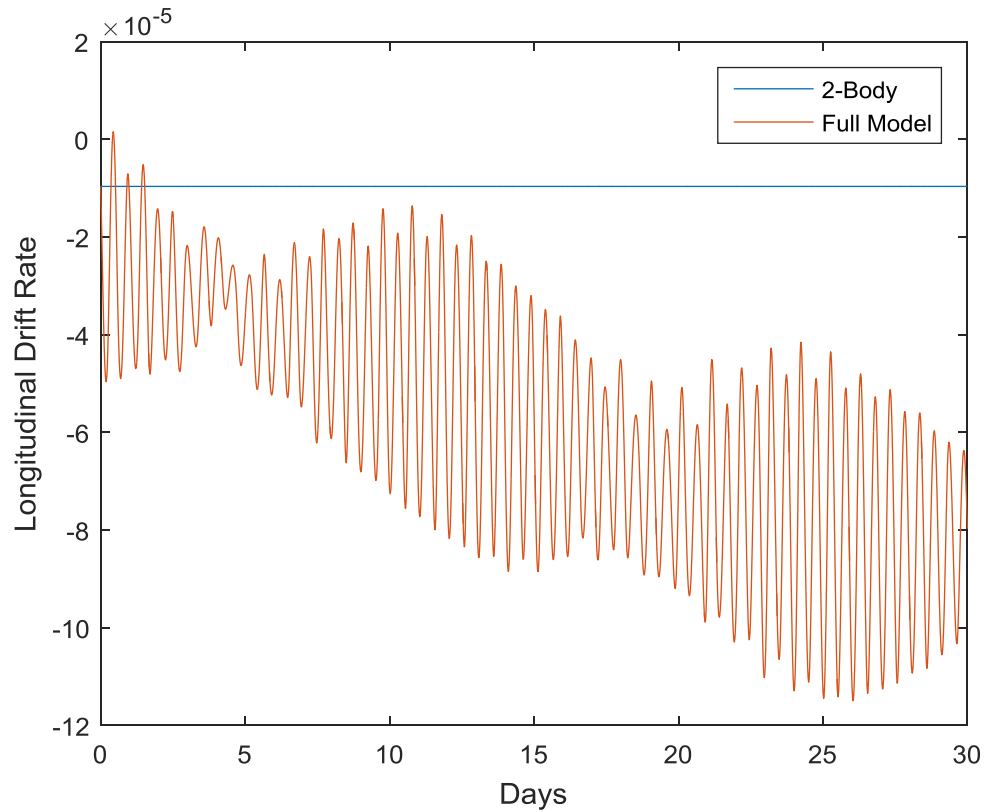
Figure 18: Perturbation Effects on Longitudinal Drift Rate.

Figure 19 shows how each of the perturbations changes the longitudinal drift rate. Most immediately, while the negative drift is entirely due to the Earth's non-homogeneous nature, the oscillations around this point are almost entirely due to the gravity from the Sun and the Moon. A constant small oscillation from the solar pressure also modifies the overall oscillation. Clearly, the Earth non-spherical harmonics can be seen driving the mean of the drift rate negative, which is the same perturbation that drove the drift of the

satellite longitude. Inspecting Equation (21), the only acceleration not considered is the northward perturbation acceleration. The radial acceleration is multiplied by the difference in *X* and *Y* direction eccentricities, whereas the tangential acceleration is multiplied by the semi-latus rectum but divided by the radius, before the two are combined. As the differences in eccentricities invariably make the radial acceleration minute in comparison, the tangential acceleration is the driving acceleration, with the radial modulating it. Similarly to the northward, the tangential perturbing acceleration is driven by the magnitude of Earth's non-spherical harmonics, steadily pulling the satellite East.
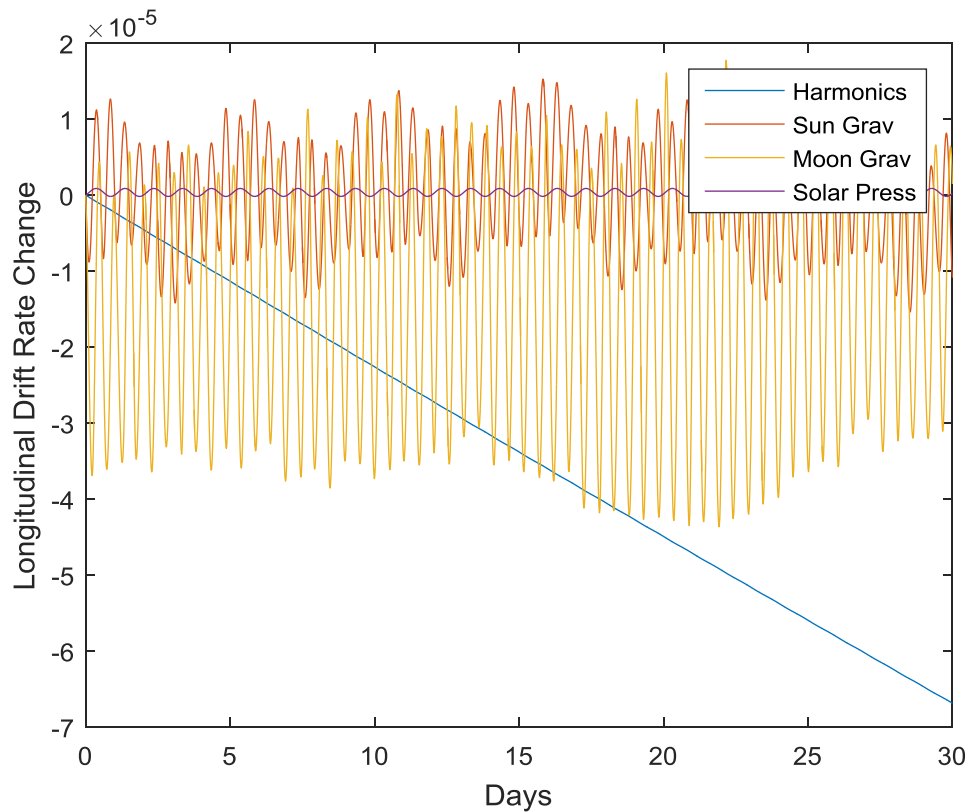
Figure 19: Longitudinal Drift Rate Perturbation Comparison.

Looking closely at how each of the other forces affects the drift rate, the Moon provides the next largest in magnitude. The perturbation from the Moon's gravity shows significant daily oscillations, which makes sense as the satellite will orbit to the opposite side of the Earth nearly once a day; however, looking closely, another periodic motion can be seen, where a half-step takes roughly 13 days. This coincides with the orbit of the Moon about the Earth. Both perturbations from the Sun have very constant oscillations. This is due to the fact that the total *change* in distance between the satellite and the Sun will change very little in relation to the total distance between the satellite and the Sun. Moving on to the eccentricity, Figure 20 displays how again the two-body model does not predict any of the changes seen. Instead, the entirety of the change in the eccentricity comes from the perturbations shown in Figure 21. In Figure 21, it can be seen that the solar pressure gives a positive drift, whereas the Earth's non-spherical harmonics give a constant libration about a constant mean, and the Sun's gravitation gives a nearly constant libration about a different mean – with slight variations in each day. The potential errors in the solar pressure assumptions could indicate the solar pressure would drive the satellite further in its eccentricity, but likely in the same direction noted here. The gravity from the Moon is far different, and clearly drives the path seen in the actual eccentricity – both by changing the mean of the oscillations, and by creating the beat-type frequency pattern with the Sun's gravity and Earth's harmonics that causes the nodal points in the eccentricity path of the actual satellite. While the Solar Pressure effect is of a small magnitude here, over several months the solar pressure would grow quite large and then return back to zero and go negative. The solar pressure is a force that provides an oscillatory acceleration on the eccentricity, but with the period of a full year. Further,

examining Equations (22) and (23), their reliance on all three acceleration directions

indicates the interactions in eccentricity are quite complex. That said, the northward

acceleration is dwarfed by the other two, so out-of-plane forces play a small role. In the

Equatorial plane, the gravity from the Earth and the Sun will be mostly oscillatory, and

the Moon will be oscillatory at frequencies of one day and every orbit of the moon. The

solar pressure, on the other hand, will constantly push the satellite away, creating a

slowly accelerating drift. This path is non-oscillatory as the attitude of the craft is

considered to be constant in relation to the Sun, so the direction of action never changes

during the month studied.
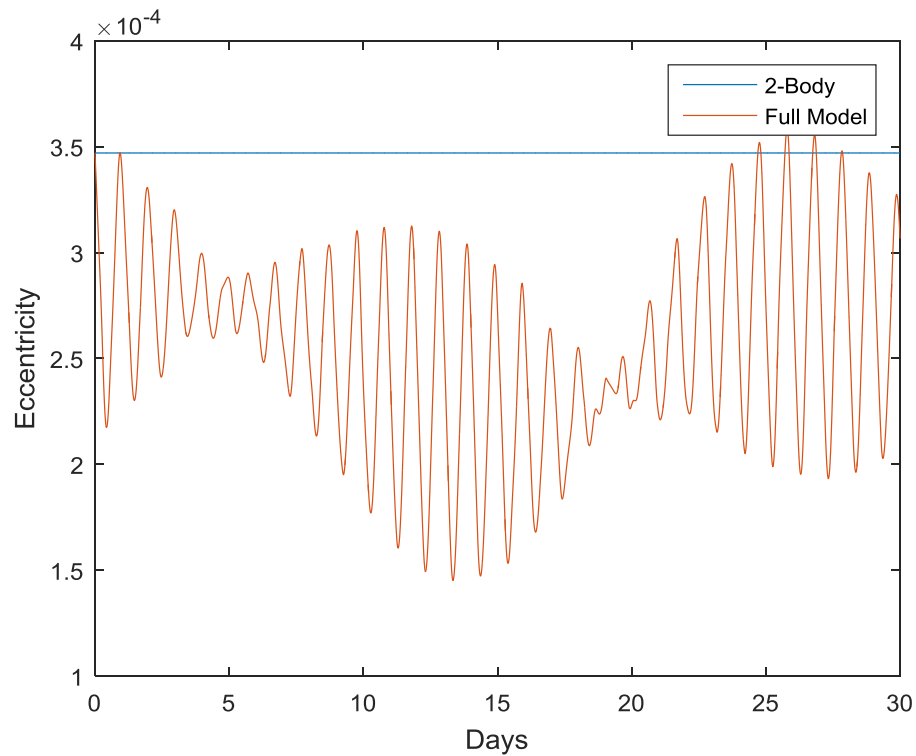
Figure 20: Perturbation Effects on Eccentricity.

Figure 22 shows that in the inclination, the 2-body model fails to create any

change. The inclination drifts entirely due to the gravitational effects of the Sun and

Moon, as shown in Figure 23. The non-spherical harmonics of the Earth, and the solar

pressure, provide no significant contributions to the change in inclination. The
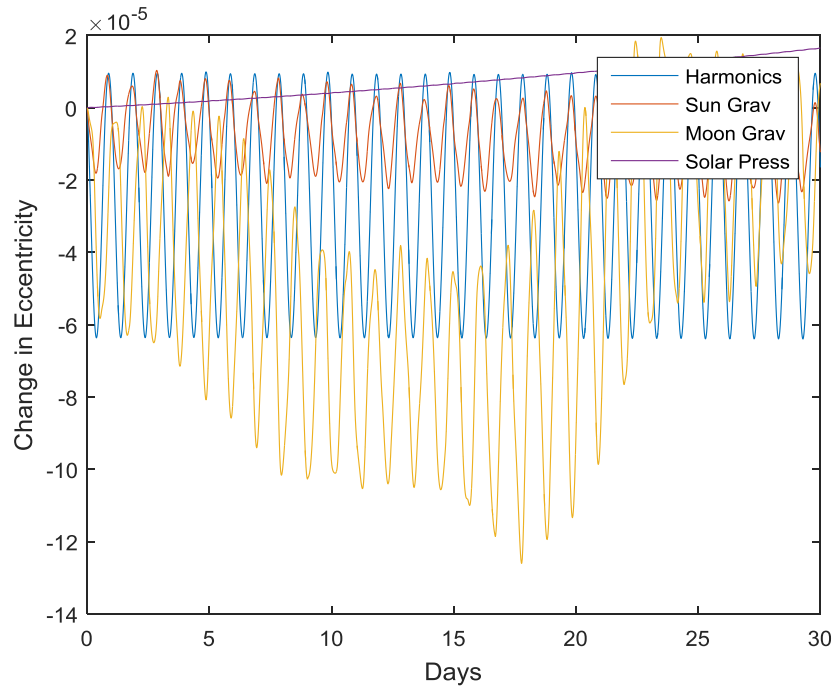
Figure 21: Eccentricity Perturbation Comparison.

long-term oscillations in the inclination are also caused entirely by the Moon. This is due

to the effect of the Moon moving closer or further from the satellite, and also being out-

of-plane of the satellite, causing the dramatic changes. The Sun is also providing an

oscillating drift pattern, as it is also getting closer and further from the satellite; however,

the vast distance to the Sun, as well as the distance changing little over a single month,

dwarfs the change in distance to the Sun, so this effect is not visible in Figure 23.

Analyzing Equations (24) and (25) for the inclination, it can be seen that the only

acceleration operating on the satellite is in the North direction – or that only out-of-plane

forces will affect it. Thus, the Earth's non-spherical harmonics and the solar pressure

both have very minimal effects; however, the Sun and the Moon, both not lying on the

same orbital plane as the satellite, pull the inclination further Northward.
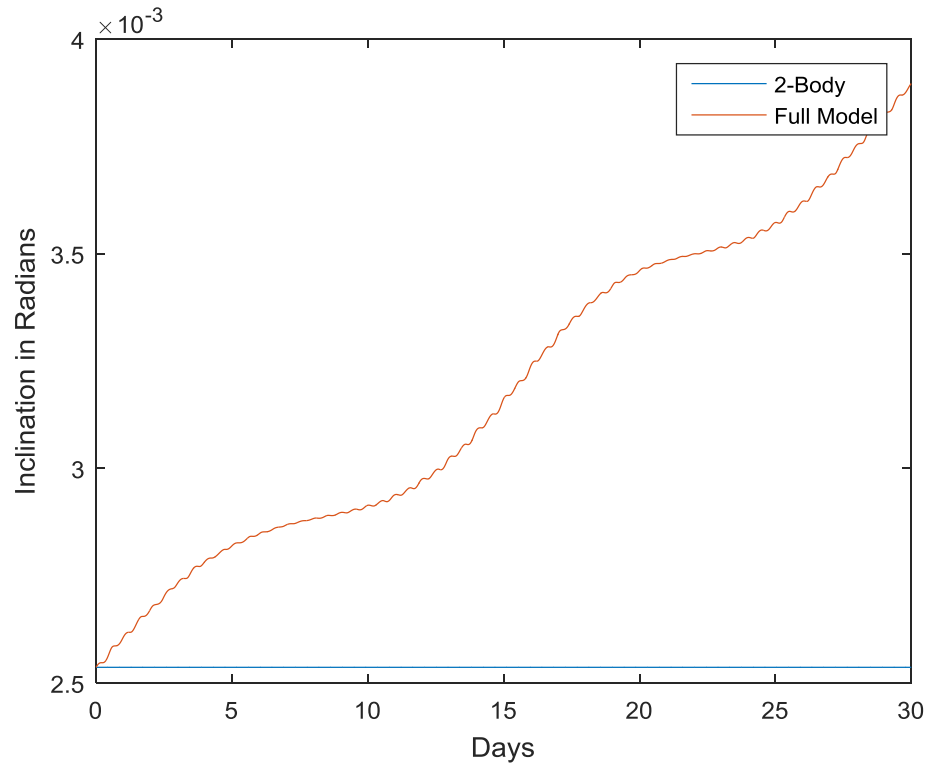
Figure 22: Perturbation Effects on Inclination.
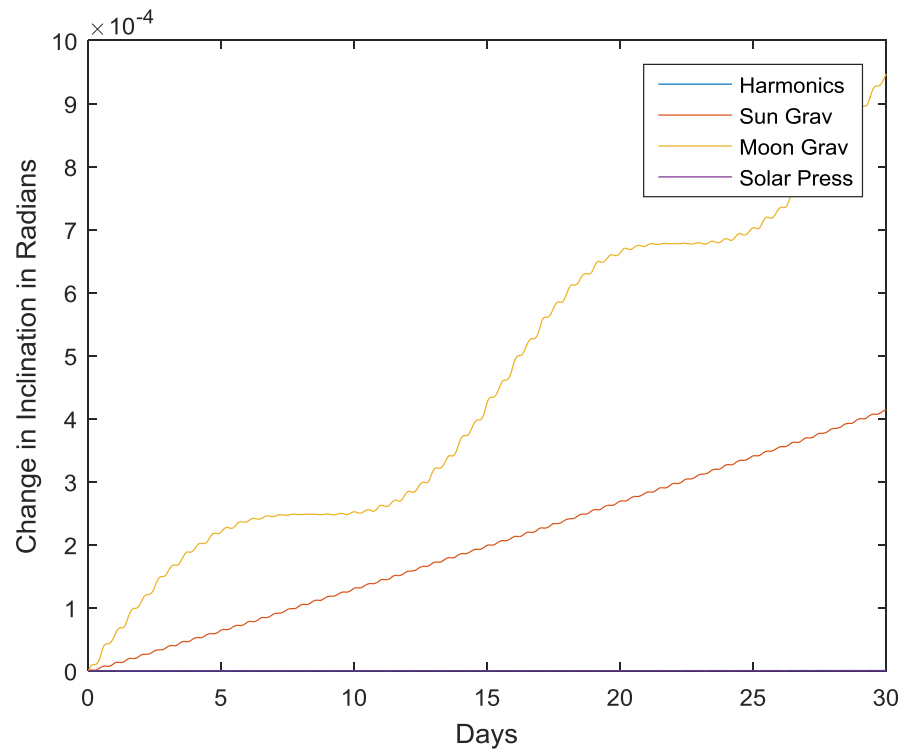
Figure 23: Inclination Perturbation Comparison.

Finally, on to the radius shown in Figure 24, it can be seen that the two-body model oscillates through a larger bound than what the fully modeled radius did. This result indicates that the changes from the perturbation forces should be largely negative on the radius. Figure 25 mostly affirms this conclusion, as even though the Sun's perturbation forces are nearly symmetrical about zero, and the Moon's gravitational force is asymmetrical about zero, the perturbation from the Earth's non-spherical harmonics are in a constant negative trend. The odd shape the radius takes comes mostly from the oscillations caused by the Moon's gravity. This effect is likely due to the changes on the eccentricity the Moon causes. The solar pressure provides a very interesting effect, as it continually spirals outward. This result shows that the Sun has a greater effect on the radius through solar pressure than through gravity. That said, the effects on the radius by all the perturbing forces are driven by the changes in the eccentricity. The solar pressure acceleration increases the satellite's oscillations further and further each day in radius, because it is pushing the eccentricity positive, as shown in Figure 21.
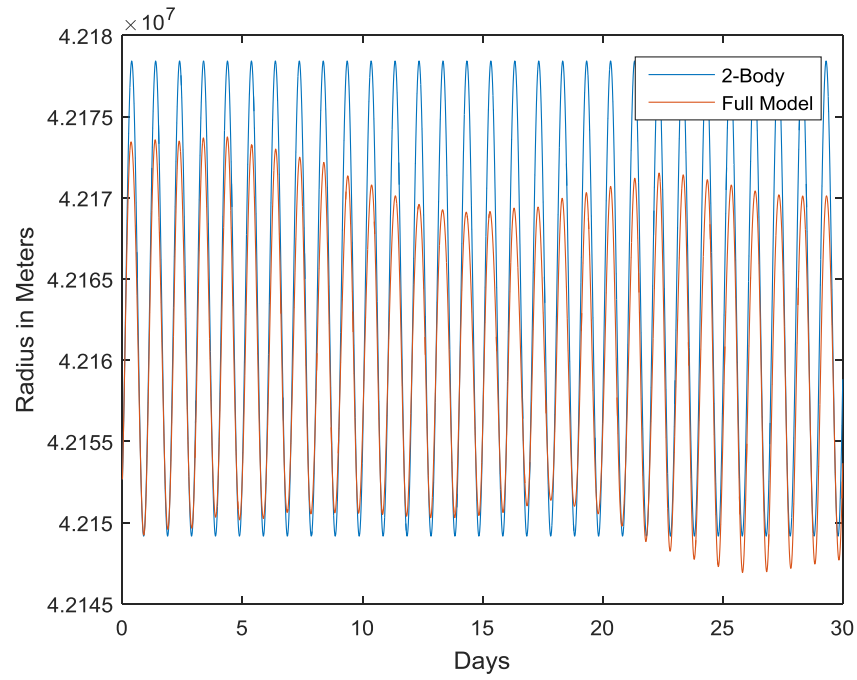
Figure 24: Perturbation Effects on Radius.
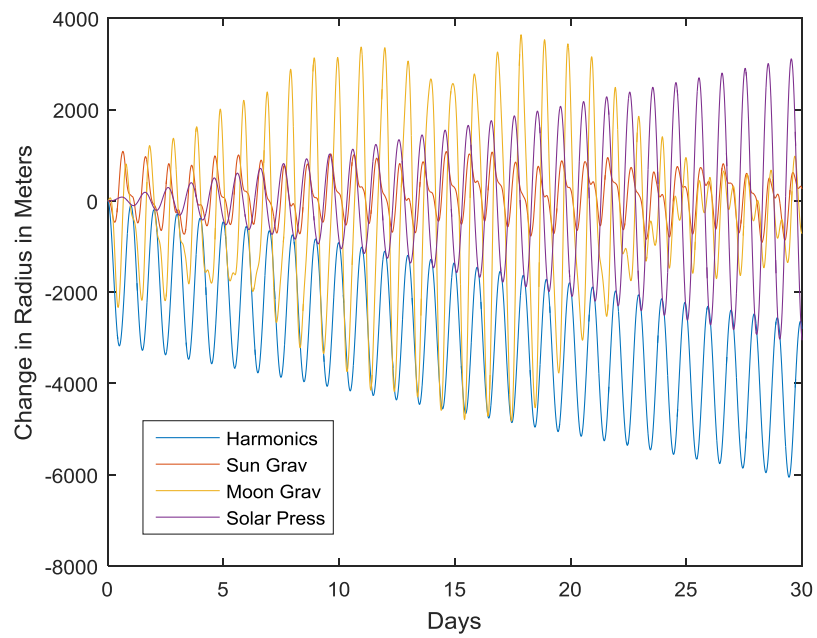
Figure 25: Radius Perturbation Comparison.

CONCLUSIONS AND RECOMMENDATIONS

Examining each perturbation in detail, the first conclusion that can easily be garnered concerns the solar pressure. While it did have a contribution in most directions, only minimally affecting the longitude and inclination, the solar pressure consistently provided the least change in the orbit – with the exception of the eccentricity and radius. While the magnitude of the change to the radius looks erroneously large, this is actually due to the solar pressure increasing the eccentricity, as shown in Figure 21. As the orbit grows more and more eccentric, the radius will have higher maximums and lower minimums, and thus the magnitude of the radius change grows as depicted in Figure 25. The remaining effects from the solar pressure are as expected, as the magnitude of the acceleration due to solar pressure is about two orders of magnitude smaller than the others. Additionally, this conclusion provides verification in the model – the model does not account for the attitude of the satellite, and the solar pressure is the only perturbation that was considered that would need to account for attitude.

Next, the effect of the moon's gravitational field is tremendous. While it is not always the largest contributing perturbation, the diurnal nature of this perturbation forces large, fluctuating oscillations in the longitudinal drift rate, eccentricity, inclination, and radius. The magnitude of this force is large, overcoming the magnitude of the Sun's gravity in every direction, especially in the inclination, and really displays how the orbit of the Moon changes everything in the GEO regime.

The acceleration due to the Sun's gravity, while still large, is considerably smaller than that from the Moon's gravity. This perturbation gave fairly constant oscillation patterns to each direction except the inclination, and a fluctuating beat-cycle to the

longitudinal drift rate. The nearly-constant oscillations are due to the relatively small changes in the distance from the satellite to the Sun from day-to-day over the course of the month studied. Concerning the inclination, the Sun's gravity would pull the satellite in a sinusoidal oscillation over a full year period; however, in this study, only one month was considered, so only a portion of this oscillation is noted.

Finally, by far the greatest perturbing force comes from the non-spherical harmonics of the Earth. Nearly controlling the entire drift of the longitude, this force is what pulled Galaxy 15 furthest from its starting position, and it caused the drift rate to accelerate throughout the month studied. That said, its contribution to the eccentricity of the orbit is significantly smaller than the contribution from the Moon. Additionally, it had no effect whatsoever on the inclination.

The perturbing forces and their principle directions of action are summarized in Table 1.

Table 1: Summary of Forces and Primary COE Over One Month.

Classical Orbital Element	Primary Perturbing Force	Secondary Perturbing Force
Longitude	Earth Non-Spherical Harmonics	Moon's Gravity
Longitudinal Drift Rate	Earth Non-Spherical Harmonics	Moon's Gravity
Eccentricity	Moon's Gravity	Solar Pressure
Inclination	Moon's Gravity	Sun's Gravity
Radius	Moon's Gravity	Solar Pressure

Comparing the actual distance the satellite drifted and the predicted distance by the model, it can be seen that initially they match entirely, but as the drift progresses past twenty days, deviations emerge. While some of the deviations are definitely due to the numerical integration and build-up of small errors, some deviation is potentially due to neglected forces, such as Venus' and Jupiter's gravitational forces, the truncation of the

spherical harmonics to eight degrees, the polynomial fits for the Sun and Moon locations, and the assumptions made for the solar pressure perturbation.

One problem that arose during the final steps of computation was the lack of computing power to run the numerical analysis to the accuracy desired for the full length of time desired. To remedy this deficiency, the numerical analysis was run for six sets of 5-day periods instead of a single 30-day period. These six sets were then combined to create the 30-day period analyzed for the specific perturbation contributions.

Future Improvements

In order to improve the analysis done here, a better attitude model for the satellite is necessary. Since the satellite information directly concerning this is not public, the best method for obtaining such information would be to estimate the reflectivity by area to mass ratio, or $\frac{c_R A_S}{m}$, from the ephemerides, and verified using an analysis of the power the solar panels were collecting. As the solar panels almost entirely govern the solar pressure on the satellite, a more accurate model would provide for a better estimate on the solar pressure actually acting on the satellite at any point in time. This process would provide for a more accurate model of the forces; however, similar conclusions as those found in this study would be expected.

Finally, the addition of smaller forces mentioned previously, such as the gravitational forces from Venus, Jupiter, and then even smaller and further elements, could be added to improve the accuracy of the model. While it would be interesting to see what contribution each of these forces has, the errors currently are very small, so it is

expected that the contributions from these neglected forces are also quite small. Yet, to

take this analysis a step further, these forces should be included.

REFERENCES

[1] Soop, E. M. 1994. *Handbook of Geostationary Orbits*. Dordrecht: Kluwer Academic.

[2] Satellites up in your Sky Right Now. No Date. [Internet, WWW]. Address: http://www.n2yo.com/whats-up/.

[3] Jansky, D. M., and Jeruchim, M. C. 1987. *Communication Satellites in the Geostationary Orbit*. Norwood, MA: Artech House.

[4] Gatland, K. W. 1964. *Telecommunication Satellites: Theory, Practice, Ground Stations, Satellites, Economics*. Englewood Cliffs, N.J;London; Iliffe Books.

[5] Weeden, B. 2011. *A Summary of the Galaxy 15 Incident and its Impact on Space Sustainability.* Secure World Foundation. [Internet, WWW, PDF]. Address: www.unoosa.org/pdf/pres/stsc2011/tech-39.pdf.

[6] Bauman, K. No Date. So This Is a Thing: Zombie Satellites. [Internet, WWW]. Address: http://www.core77.com/posts/27196/So-This-Is-a-Thing-Zombie-Satellites.

[7] Enge, P. K., and Van Dierendonck, A. J. 1996. "Wide Area Augmentation System." *Progress in Astronautics and Aeronautics*, *164*, pp. 117-142.

[8] Reigber, C., Schwintzer, P., Neumayer, K. H., Barthelmes, F., König, R., Förste, C., ... and Bruinsma, S. 2003. "The CHAMP-only Earth Gravity Field Model EIGEN-2." *Advances in Space Research*, *31*(8), pp. 1883-1888.

[9] Musen, P. 1960. "The Influence of the Solar Radiation Pressure on the Motion of an Artificial Satellite." *Journal of Geophysical Research,* Vol. 65 (5), pp. 1391-

1396. [Internet, WWW, PDF]. *Available* Available from the NASA website; Address: http://ntrs.nasa.gov/archive/nasa/casi.ntrs.nasa.gov/20150019717.pdf.

[10] Borovsky, J. E., and Denton, M. H. (2010). "Magnetic Field at Geosynchronous Orbit During High-Speed Stream-Driven Storms: Connections to the Solar Wind, the Plasma Sheet, and the Outer Electron Radiation Belt." *Journal of Geophysical Research. Space Physics, 115*(8), pp. [1] - [35]. [Internet, WWW]. Address: http://dx.doi.org/10.1029/2009JA015116.

[11] Bobojc, A., and Droyner, A. 2011. "GOCE Satellite Orbit in the Aspect of Selected Gravitational Perturbations." *Acta Geophysica, 59*(2), pp. 428-452. [Internet, WWW]. Address: http://dx.doi.org/10.2478/s11600-010-0052-3

[12] Aslanov, V. S., Ledkov, A. S., Misra, A. K., and Guerman, A. D. 2013. "Dynamics of Space Elevator After Tether Rupture." *Journal of Guidance, Control, and Dynamics*, *36*(4), pp. 986-992. [Internet, WWW]. Address: http://dx.doi.org/10.2514/1.59378.

[13] Wee, L. K., and Goh, G. H. 201. "A Geostationary Earth Orbit Satellite Model Using Easy Java Simulation." *Physics Education, 48*(1), pp. 72 - 79. [Internet, WWW]. Address: http://dx.doi.org/10.1088/0031-9120/48/1172.

[14] Yoon, J., Lee, K., Lee, B., Kim, B., Choi, K., Chang, Y. Ra, S. 2004. "Geostationary Orbit Determination for Time Synchronization Using Analytical Dynamic Models." *IEEE Transactions on Aerospace and Electronic Systems, 40*(4), pp. 1132-1146. [Internet, WWW]. Address: http://dx.doi.org/10.1109/TAES.2004.1386869.

[15] Cliverd, Mark A. *et al*. 2012 "Energetic Particle Injection, Acceleration, and Loss during the Geomagnetic Disturbances Which Upset Galaxy 15." *Journal of Geophysical Research. Space Physics* 117 (12), pp. [1] − [16]. [Internet, WWW]. Address: http:dx.doi.org/10.1029/2012ja018175.

[16] "Intelsat Restores Power to Galaxy 15; Recovery Efforts Underway." 2010. *Satellite Today* Vol. 9, p. 248 [Internet, WWW, Database]. Address: http://www.proquest.com/

[17] "Intelsat; Galaxy 15 Commercial Customers to Transition to Galaxy 12 Following Anomaly." 2010. *Telecommunications Weekly* p. 236. [Internet, WWW]. Address: http://www.proquest.com/

[18] Shallberg, Karl, Potter, B.J., and Class, Phillip. "Geostationary Satellite Reference Station Multipath Characterization: Using Galaxy 15 Failure to Refine the WAAS Multipath Threat." *24th International Technical Meeting of the Satellite Division of the Institute of Navigation 2011, ION GNSS 2011,* v4, pp. [2453]-[2461].

[19] Lafleur, C. 5 April 2010. Spacecraft Stats and Insights. [Internet, WWW]. Address: http://www.thespacereview.com/article/1598/1

[20] Satbeams - World of Satellites at Your Fingertips. No Date. [Internet, WWW]. Address: http://www.satbeams.com/satellites

[21] Vallado, D. A., and McClain, W. D. 2001. *Fundamentals of Astrodynamics and Applications* (3rd ed.). Dordrecht: Kluwer Academic.

[22] Perturbed Motion. No Date. [Internet, WWW]. Address: http://www.navipedia.net/index.php/Perturbed_Motion

[23] Newton, Sir Isaac. 1687, 1934. *Sir Isaac Newton's Mathematical* "Principles of Natural Philosophy and his System of the World." Berkeley, CA: University of California Press.

[24] Tombasco, J., Axelrad, P., and Jah, M. 2010. "Specialized Coordinate Representation for Dynamic Modeling and Orbit Estimation of Geosynchronous Orbits." *Journal of Guidance, Control, and Dynamics, 33*(6), pp. 1824-1836. [Internet, WWW]. Address: http://dx.doi/org/10.2514/1.48903

[25] Grace Recovery and Climate Experiment. 2008. [Internet, WWW]. Address: http://www.csr.utexas.edu/grace/gravity/

[26] Shea, S. P. 2012 "Evaluation of Glare Potential for Photovoltaic Installations." [Internet, WWW]. Address: http://www.suniva.com/documents/Suniva%20Reflection%20and%20Glare%20Report%20-%20Marketing%20-%20August%202012.pdf

[27] NASA's Juno Spacecraft Breaks Solar Power Distance Record. 2016/ [Internet, WWW]. Address: http://www.jpl.nasa.gov/news/news.php?feature=4818

[28] StarChild Question of the Month for April 2001. [Internet, WWW]. Address: https://starchild.gsfc.nasa.gov/docs/StarChild/questions/question32.html

[29] Federal Aviation Administration. No Date. [Internet, WWW]. Address: http://www.nstb.tc.faa.gov/DisplayNSTBDataDownload.htm

Appendix A

Legendre Polynomials

The Legendre Polynomial, represented by Equation (A1), is utilized to codify a sphere into specific sections. The polynomial, $P_{l,m}[\gamma]$ will create ever-smaller portions with higher values of l. Here, l and m are merely counters, where l will rise to infinity, and m will rise from 0 to l for each value of l. This means, for an l value of 2, three P polynomials are obtained, $P_{2,0}$, $P_{2,1}$, and $P_{2,2}$. The Legendre Polynomial is given by[1]

$$P_{l,m}[\gamma] = \frac{1}{2^l l!}(1 - \gamma^2)^{m/2} \frac{d^{l+m}}{d\gamma^{l+m}}(\gamma^2 - 1)^l. \tag{A1}$$

For gravitational spherical harmonics, the variable γ is replaced by $\sin \phi$, so the equation becomes

$$P_{l,m}[\sin \phi] = \frac{1}{2^l l!}(1 - \sin \phi^2)^{m/2} \frac{d^{l+m}}{d \sin \phi^{l+m}}(\sin \phi^2 - 1)^l. \tag{A2}$$

This means for each new value of l, a new equation is obtained to take derivatives of, but for each value of m at the same value of l, another derivative of the same equation is simply taken. Vallado and McClain[1] present the polynomials for $l=0$ to 4, so this will only consider the evaluation of the values $l=5$ to 8.

Taking Equation (A2) in two halves, the expression can simplify quite easily. The first portion becomes

$$\frac{(\cos \phi^2)^{m/2}}{2^l l!} = \frac{\cos \phi^m}{2^l l!},$$

which is fairly simple to evaluate for m and l; however, it changes with changing ϕ. For $l=5$, this gives us, with m going from 1 to 5

$$\frac{\cos \phi^m}{3840}.$$

Next, $l=6$ through 8 is shown in the following line:

$$\frac{\cos \phi^m}{46080}; \frac{\cos \phi^m}{645120}; \frac{\cos \phi^m}{10321920}.$$

[1]Vallado, D.A. and McClain, W.D. 2001. *Fundamentals of Astrodynamics and Applications* (3rd ed.). Dordrecth: Kluwer Academic

Thus, it becomes obvious why this is only considered through $l=8$ – any further and the contribution becomes miniscule, though not insignificant for precise orbit determination. The second half of Equation (A1) is more difficult, but with some simplification, it too is not impossible. Replacing $\sin \phi$ with x gives:

$$\frac{d^{l+m}}{d \sin \phi^{l+m}} (\sin \phi^2 - 1)^l = \frac{d^{l+m}}{dx^{l+m}} (x^2 - 1)^l, \tag{A3}$$

which becomes, for $l=5$ to 8, respectively:

$$\frac{d^{5+m}}{dx^{5+m}} (x^2 - 1)^5 = \frac{d^{5+m}}{dx^{5+m}} (x^{10} - 5x^8 + 10x^6 - 10x^4 + 5x^2 - 1), \tag{A4}$$

$$\frac{d^{6+m}}{dx^{6+m}} (x^2 - 1)^6 = \frac{d^{6+m}}{dx^{6+m}} (x^{12} - 6x^{10} + 15x^8 - 20x^6 + 15x^4 - 6x^2 + 1), \tag{A5}$$

$$\frac{d^{7+m}}{dx^{7+m}} (x^2 - 1)^7 = \frac{d^{7+m}}{dx^{7+m}} (x^{14} - 7x^{12} + 21x^{10} - 35x^8 + 35x^6 - 21x^4 + 7x^2 - $$

$$1), \tag{A6}$$

and

$$\frac{d^{8+m}}{dx^{8+m}} (x^2 - 1)^8 = \frac{d^{8+m}}{dx^{8+m}} (x^{16} - 8x^{14} + 28x^{12} - 56x^{10} + 70x^8 - 56x^6 + 28x^4 - $$

$$8x^2 + 1). \tag{A7}$$

Since the derivatives of Equation (A4) start at the 5th degree, only the 5th through 10th derivatives are needed; these are, when combined with the first half of the polynomial above:

$$\frac{1}{3840} (30240 \sin \phi^5 - 33600 \sin \phi^3 + 7200 \sin \phi),$$

$$\frac{\cos \phi}{3840} (151200 \sin \phi^4 - 100800 \sin \phi^2 + 7200),$$

$$\frac{\cos \phi^2}{3840} (604800 \sin \phi^3 - 201600 \sin \phi),$$

$$\frac{\cos \phi^3}{3840} (1814400 \sin \phi^2 - 201600),$$

$$945 \sin \phi \cos \phi^4,$$

and

$$945 \cos \phi^5.$$

Similarly, for *l=6*, the following polynomials form:

$$\frac{1}{46080}(665280 \sin \phi^6 - 907200 \sin \phi^4 + 302400 \sin \phi^2 - 14400),$$

$$\frac{\cos \phi}{46080}(3991680 \sin \phi^5 - 3628800 \sin \phi^3 + 604800 \sin \phi),$$

$$\frac{\cos \phi^2}{46080}(19958400 \sin \phi^4 - 10886400 \sin \phi^2 + 604800),$$

$$\frac{\cos \phi^3}{46080}(79833600 \sin \phi^3 - 21772800 \sin \phi)$$

$$\frac{\cos \phi^4}{46080}(239500800 \sin \phi^2 - 21772800),$$

$$10395 \sin \phi \cos \phi^5,$$

and

$$10395 \cos \phi^6.$$

Similarly, for *l=7*, the following polynomials form:

$$\frac{1}{645120}(17297280 \sin \phi^7 - 27941760 \sin \phi^5 + 12700800 \sin \phi^3 - 1411200 \sin \phi),$$

$$\frac{\cos \phi}{645120}(121080960 \sin \phi^6 - 139708800 \sin \phi^4 + 38102400 \sin \phi^2 - 1411200),$$

$$\frac{\cos \phi^2}{645120}(726485760 \sin \phi^5 - 558835200 \sin \phi^3 + 76204800 \sin \phi),$$

$$\frac{\cos \phi^3}{645120}(3632428800 \sin \phi^4 - 1676505600 \sin \phi^2 + 76204800),$$

$$\frac{\cos \phi^4}{645120}(14529715200 \sin \phi^3 - 3353011200 \sin \phi)$$

$$\frac{\cos \phi^5}{645120}(43589145600 \sin \phi^2 - 3353011200),$$

$$135135 \sin \phi \cos \phi^6,$$

and

$$135135 \cos \phi^7.$$

Similarly, for *l=8*, the following polynomials form:

$$\frac{1}{10321920} (518918400 \sin \phi^8 - 968647680 \sin \phi^6 + 558835200 \sin \phi^4 -$$

$$101606400 \sin \phi^2 + 2822400),$$

$$\frac{\cos \phi}{10321920} (4151347200 \sin \phi^7 - 5811886080 \sin \phi^5 + 2235340800 \sin \phi^3 -$$

$$203212800 \sin \phi),$$

$$\frac{\cos \phi^2}{10321920} (29059430400 \sin \phi^6 - 29059430400 \sin \phi^4 + 6706022400 \sin \phi^2 -$$

$$203212800),$$

$$\frac{\cos \phi^3}{10321920} (174356582400 \sin \phi^5 - 116237721600 \sin \phi^3 + 13412044800 \sin \phi),$$

$$\frac{\cos \phi^4}{10321920} (871782912000 \sin \phi^4 - 348713164800 \sin \phi^2 + 13412044800),$$

$$\frac{\cos \phi^5}{10321920} (3487131648000 \sin \phi^3 - 697426329600 \sin \phi)$$

$$\frac{\cos \phi^6}{10321920} (10464394944000 \sin \phi^2 - 697426329600),$$

$$2027025 \sin \phi \cos \phi^7,$$

and

$$2027025 \cos \phi^8.$$

Appendix B

Matlab® Code

```matlab
% This program sets up the model for a spacecraft in circular planar
orbit
% about Earth at the geosynchronous altitude

% David P. Schafer
% 11/27/2016

close all
clear x t lambda deltaA Ex Ey Ix Iy Ecc Inc g s r
clc
global G0 A mu we

G0 = 3.8314;
we = .00007292115;%85; % Rotational velocity of the Earth in radians
per sec
mu = 3.986004418*10^14; % Gravity! in m^3/s^2
A = 42164200; % Semi-major axis in m
tspan = 0:(86400*5);
lam0 = -2.315341310053890; % initial longitude - ECEF
delA = -9.646508181568860e-06; % ECI data
ex = 2.392198936783866e-04;
ey = 2.513727391392481e-04;
ix = 0.002504178455663;
iy = -4.047830759746088e-04;


x0 = [lam0;delA;ex;ey;ix;iy];


[t,x] = ode45('deltax', tspan, x0);


y0 = [x(end,1);x(end,2);x(end,3);x(end,4);x(end,5);x(end,6)];


[tt,y] = ode45('deltax', tspan + 86400*5, y0);


z0 = [y(end,1);y(end,2);y(end,3);y(end,4);y(end,5);y(end,6)];


[ttt,z] = ode45('deltax', tspan + 86400*10, z0);


a0 = [z(end,1);z(end,2);z(end,3);z(end,4);z(end,5);z(end,6)];


[tttt,a] = ode45('deltax', tspan + 86400*15, a0);


b0 = [a(end,1);a(end,2);a(end,3);a(end,4);a(end,5);a(end,6)];


[ttttt,b] = ode45('deltax', tspan + 86400*20, b0);


c0 = [b(end,1);b(end,2);b(end,3);b(end,4);b(end,5);b(end,6)];


[tttttt,c] = ode45('deltax', tspan + 86400*25, c0);

t = [t;tt;ttt;tttt;ttttt;tttttt];
lambda = [x(:,1);y(:,1);z(:,1);a(:,1);b(:,1);c(:,1)];
deltaA = [x(:,2);y(:,2);z(:,2);a(:,2);b(:,2);c(:,2)];
Ex = [x(:,3);y(:,3);z(:,3);a(:,3);b(:,3);c(:,3)];
Ey = [x(:,4);y(:,4);z(:,4);a(:,4);b(:,4);c(:,4)];
```

```matlab
Ix = [x(:,5);y(:,5);z(:,5);a(:,5);b(:,5);c(:,5)];
Iy = [x(:,6);y(:,6);z(:,6);a(:,6);b(:,6);c(:,6)];
for i = 1:length(Ex)
Ecc(i) = sqrt(Ex(i)^2 + Ey(i)^2);
Inc(i) = sqrt(Ix(i)^2 + Iy(i)^2);
g(i) = G0 + we*t(i);
s(i) = lambda(i) + g(i);
r(i) = A*(deltaA(i) + 1)*(1 - Ex(i)^2 - Ey(i)^2)/(1 + Ex(i)*cos(s(i)) +
Ey(i)*sin(s(i)));
end
t = t/86400.002;

plot(t,lambda*180/pi)
xlabel('Days');
ylabel('Longitude in Degrees');

% figure
% plot(t,deltaA)
% xlabel('Time (Days)');
% ylabel('Longitudinal Drift Rate');
%
% figure
% plot(t,Ecc)
% xlabel('Days');
% ylabel('Eccentricity');
%
% figure
% plot(t,Inc)
% xlabel('Days');
% ylabel('Inclination');
%
% figure
% plot(t,r)
% xlabel('Days');
% ylabel('Radius');
```

```matlab
function dxdt = deltax(t,x)

% David P. Schafer
% 11/27/2016

format long

global G0 we A mu
a = [0,0,0];
lam = x(1); % ECEF
dela = x(2); % ECI
ex = x(3);
ey = x(4);
ix = x(5);
iy = x(6);
inc = sqrt(ix^2 + iy^2);
ecc = sqrt(ex^2 + ey^2);
g = G0 + we*t;
while g > 2*pi
    g = g-2*pi;
end
OHM = -atan(ix/iy);
ohm = atan(ey/ex) - OHM;

as = 20; % surface area of satellite? m*m
cr = 1.35; % reflectivity of solar panels
psr = 4.56*10^-6; % N/m*m
msat = 2000; % mass of satellite, kg

nu = lam + 1*g - ohm - OHM;

mus = 1.32712440018*10^20; % mu of sun - m^3/s^2
mum = 4.9048695*10^12; % mu of moon - m^3/s^2
%%

s = lam + g;
while s > 2*pi
    s = s - 2*pi;
end

r = A*(dela + 1)*(1 - ex^2 - ey^2)/(1 + ex*cos(s) + ey*sin(s));
p = A*(dela + 1)*(1 - ex^2 - ey^2);
h = sqrt(mu*p);

Q1 = tan(inc/2)*sin(OHM);
Q2 = tan(inc/2)*cos(OHM);
QQ = [(1 + Q2^2 - Q1^2)*cos(s) + 2*Q1*Q2*sin(s);(1 + Q1^2 -
Q2^2)*sin(s) + 2*Q1*Q2*cos(s); 2*(Q2*sin(s) - Q1*cos(s))];

rr = (r/(1 + Q1^2 + Q2^2))*QQ; % Dr. Seubert eq. 12 - eci

rotate = [cos(OHM)*cos(ohm) - sin(OHM)*sin(ohm)*cos(inc), -
cos(OHM)*sin(ohm) - sin(OHM)*cos(ohm)*cos(inc), sin(OHM)*sin(inc);
```

```
sin(OHM)*cos(ohm) + cos(OHM)*sin(ohm)*cos(inc), -sin(OHM)*sin(ohm) +
cos(OHM)*cos(ohm)*cos(inc), -cos(OHM)*sin(inc); sin(ohm)*sin(inc),
cos(ohm)*sin(inc), cos(inc)];
r2 = rotate*[p*cos(nu)/(1 + ecc*cos(nu)); p*sin(nu)/(1 + ecc*cos(nu));
0];
v = rotate*[-(mu/p)^.5*sin(nu); (mu/p)^.5*(ecc + cos(nu)); 0];


ener = norm(v)^2/2 - mu/r;
deltaa = (-mu/(2*ener)-A)/A;


ecchange = [cos(g), -sin(g), 0; sin(g), cos(g), 0; 0, 0, 1];
rrecef = ecchange\rr;
vvecef = ecchange\v;
recef = sqrt(dot(rrecef,rrecef));


% ph = asin(rrecef(3)/recef);
ph = atan(rrecef(3)/sqrt(rrecef(2)^2 + rrecef(1)^2));


%stime = linspace(-.5*2*pi/365.25,2*pi*30.5/365.25,86400*31+1);
stime = linspace(0,2*pi*31/365.25,86400*31+1);
ps = 1*10^11*[0.000000001231397  -0.000000028192536   0.000000220724496
-0.000000696110680   0.000002527565454 0.000054714775399  -
0.002935660657598  -0.068363221183367   1.147958294850282];
sss = polyval(ps,stime);
ps2 = 1*10^10*[0.000000010577885  -0.000000346859404
0.000004281092874  -0.000024314276274   0.000076908243913 -
0.000744005026443  -0.022657979025645   0.760359730095780
8.959090128011694];
ss2 = polyval(ps2,stime);
ps3 = 1*10^10*[0.000000006050615  -0.000000186475963
0.000002176867466  -0.000011798093022   0.000036284704353 -
0.000332000227120  -0.009810180895705   0.329672921952460
3.883925232122224];
ss3 = polyval(ps3,stime);
res = [sss(floor(t+1)); ss2(floor(t+1)); ss3(floor(t+1))]; % earth to
sun
%res = ersun(t);
rs = res - rr; % define sat to sun


%mtime = linspace(-.5*2*pi/27.322,2*pi*30.5/27.322,86400*31+1);
mtime = linspace(0,2*pi*31/27.322,86400*31+1);
pm = 1*10^8*[0.000101327109054  -0.002319929681139   0.018167291807621
-0.055800313738517   0.114946027844420 -0.562297318378231
0.427725810332882   3.516129197912261  -1.216399516612842];
mmm = polyval(pm,mtime);
pm2 = 1*10^8*[0.000087050522716  -0.002854658384220   0.035251819897064
-0.201130690491850   0.545894068041208 -0.979490407031079
2.424549911936519  -1.668444060540370  -3.257784162975650];
mm2 = polyval(pm2,mtime);
pm3 = 1*10^8*[0.000049794010890  -0.001534686225960   0.017923344013322
-0.097540035664799   0.260870706445225 -0.502417542439565
1.154148301823466  -0.431551168407016  -1.609681950477247];
mm3 = polyval(pm3,mtime);
rem = [mmm(floor(t+1)); mm2(floor(t+1)); mm3(floor(t+1))]; % define
earth to moon
%rem = ermoon(t);
```

```
rm = rem - rr; % define sat to moon

ea = [0;0;0];
es = 0;
em = 0;
esp = 0;

ell = ellipsoidal(r,ph,lam,rrecef);

ea = ecchange*ell;  % rotated to inertial here
es = mus*(rs/norm(rs)^3 - res/norm(res)^3); %
em = mum*(rm/norm(rm)^3 - rem/norm(rem)^3); %
esp = (-psr*cr*as/msat)*(rs/sqrt(dot(rs,rs))); % x2 inertial frame
radiation pressure
a = ea + es + em + esp;
%% rotate from earth-centered inertial to satellite body-fixed here
(LVLH)
RR = rr/sqrt(dot(rr,rr));
WW = cross(rr,v)/sqrt(dot(cross(rr,v),cross(rr,v)));
SS = cross(WW,RR);
rot = [RR,SS,WW];
a = rot\a;
%%

dlamdt = h/r^2 + (r/h)*tan(inc/2)*sin(ohm + nu)*a(3) - we;

ddeltaa = (A*(2*(dela + 1)^2)/(h))*((ex*sin(s) - ey*cos(s))*a(1) +
p*a(2)/r);

dex = (r/h)*((p/r)*sin(s)*a(1) + (ex + (1 + (p/r))*cos(s))*a(2)) +
ey*(r/h)*((tan(inc/2)*sin(OHM)*cos(s) -
tan(inc/2)*cos(OHM)*sin(s))*a(3));
dey = (r/h)*((-p/r)*cos(s)*a(1) + (ey + (1 + (p/r))*sin(s))*a(2)) -
ex*(r/h)*((tan(inc/2)*sin(OHM)*cos(s) -
tan(inc/2)*cos(OHM)*sin(s))*a(3));
dix = ((r/h)*sin(OHM)*cos(ohm + nu) +
(inc*r/(h*sin(inc)))*cos(OHM)*sin(ohm + nu))*a(3);
diy = ((inc*r/(h*sin(inc)))*sin(OHM)*sin(ohm + nu) -
(r/h)*cos(OHM)*cos(ohm + nu))*a(3);

dxdt = [dlamdt;ddeltaa;dex;dey;dix;diy];
```
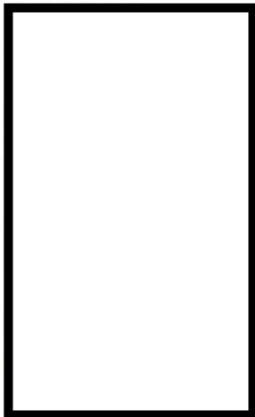
Appendix C

Copyrighted Works Use Agreements

SPRINGER LICENSE
TERMS AND CONDITIONS

Oct 09, 2016

This Agreement between David P Schafer ("You") and Springer ("Springer") consists of your license details and the terms and conditions provided by Springer and Copyright Clearance Center.

License Number	3964870847589
License date	Oct 09, 2016
Licensed Content Publisher	Springer
Licensed Content Publication	Celestial Mechanics and Dynamical Astronomy
Licensed Content Title	Handbook of geostationary orbits
Licensed Content Author	B. G. Williams
Licensed Content Date	Jan 1, 1997
Licensed Content Volume Number	65
Licensed Content Issue Number	4
Type of Use	Thesis/Dissertation
Portion	Figures/tables/illustrations
Number of figures/tables/illustrations	3
Author of this Springer article	No
Order reference number	
Original figure numbers	Figure 2.1.C, 2.1.D, and 4.4.A
Title of your thesis / dissertation	Examining Forces at Geostationary Orbit with Galaxy 15 Uncontrolled Wide Area Augmentation System Ephemerides
Expected completion date	Nov 2016
Estimated size(pages)	60
Requestor Location	
Billing Type	
Billing Address	
Total	
Terms and Conditions	

Introduction

The publisher for this copyrighted material is Springer. By clicking "accept" in connection with completing this licensing transaction, you agree that the following terms and conditions apply to this transaction (along with the Billing and Payment terms and conditions established by Copyright Clearance Center, Inc. ("CCC"), at the time that you opened your Rightslink account and that are available at any time at http://myaccount.copyright.com).

Limited License

With reference to your request to reuse material on which Springer controls the copyright, permission is granted for the use indicated in your enquiry under the following conditions:

- Licenses are for one-time use only with a maximum distribution equal to the number stated in your request.

- Springer material represents original material which does not carry references to other sources. If the material in question appears with a credit to another source, this permission is not valid and authorization has to be obtained from the original copyright holder.

- This permission

• is non-exclusive

• is only valid if no personal rights, trademarks, or competitive products are infringed.

• explicitly excludes the right for derivatives.

- Springer does not supply original artwork or content.

- According to the format which you have selected, the following conditions apply accordingly:

• **Print and Electronic:** This License include use in electronic form provided it is password protected, on intranet, or CD-Rom/DVD or E-book/E-journal. It may not be republished in electronic open access.

• **Print:** This License excludes use in electronic form.

• **Electronic:** This License only pertains to use in electronic form provided it is password protected, on intranet, or CD-Rom/DVD or E-book/E-journal. It may not be republished in electronic open access.

For any electronic use not mentioned, please contact Springer at permissions.springer@spi-global.com.

- Although Springer controls the copyright to the material and is entitled to negotiate on rights, this license is only valid subject to courtesy information to the author (address is given in the article/chapter).

- If you are an STM Signatory or your work will be published by an STM Signatory and you are requesting to reuse figures/tables/illustrations or single text extracts, permission is granted according to STM Permissions Guidelines: http://www.stm-assoc.org/permissions-guidelines/

For any electronic use not mentioned in the Guidelines, please contact Springer at permissions.springer@spi-global.com. If you request to reuse more content than stipulated in the STM Permissions Guidelines, you will be charged a permission fee for the excess content.

Permission is valid upon payment of the fee as indicated in the licensing process. If permission is granted free of charge on this occasion, that does not prejudice any rights we might have to charge for reproduction of our copyrighted material in the future.

-If your request is for reuse in a Thesis, permission is granted free of charge under the following conditions:

This license is valid for one-time use only for the purpose of defending your thesis and with a maximum of 100 extra copies in paper. If the thesis is going to be published, permission needs to be reobtained.

- includes use in an electronic form, provided it is an author-created version of the thesis on his/her own website and his/her university's repository, including UMI (according to the definition on the Sherpa website: http://www.sherpa.ac.uk/romeo/);

- is subject to courtesy information to the co-author or corresponding author.

Geographic Rights: Scope

Licenses may be exercised anywhere in the world.

Altering/Modifying Material: Not Permitted

Figures, tables, and illustrations may be altered minimally to serve your work. You may not alter or modify text in any manner. Abbreviations, additions, deletions and/or any other alterations shall be made only with prior written authorization of the author(s).

Reservation of Rights

Springer reserves all rights not specifically granted in the combination of (i) the license details provided by you and accepted in the course of this licensing transaction and (ii) these terms and conditions and (iii) CCC's Billing and Payment terms and conditions.

License Contingent on Payment

While you may exercise the rights licensed immediately upon issuance of the license at the end of the licensing process for the transaction, provided that you have disclosed complete and accurate details of your proposed use, no license is finally effective unless and until full payment is received from you (either by Springer or by CCC) as provided in CCC's Billing and Payment terms and conditions. If full payment is not received by the date due, then any license preliminarily granted shall be deemed automatically revoked and shall be void as if never granted. Further, in the event that you breach any of these terms and conditions or any of CCC's Billing and Payment terms and conditions, the license is automatically revoked and shall be void as if never granted. Use of materials as described in a revoked license, as well as any use of the materials beyond the scope of an unrevoked license, may constitute copyright infringement and Springer reserves the right to take any and all action to protect its copyright in the materials.

Copyright Notice: Disclaimer

You must include the following copyright and permission notice in connection with any reproduction of the licensed material:

"Springer book/journal title, chapter/article title, volume, year of publication, page, name(s) of author(s), (original copyright notice as given in the publication in which the material was originally published) "With permission of Springer"

In case of use of a graph or illustration, the caption of the graph or illustration must be included, as it is indicated in the original publication.

Warranties: None

Springer makes no representations or warranties with respect to the licensed material and adopts on its own behalf the limitations and disclaimers established by CCC on its behalf in its Billing and Payment terms and conditions for this licensing transaction.

Indemnity

You hereby indemnify and agree to hold harmless Springer and CCC, and their respective officers, directors, employees and agents, from and against any and all claims arising out of your use of the licensed material other than as specifically authorized pursuant to this license.

No Transfer of License

This license is personal to you and may not be sublicensed, assigned, or transferred by you without Springer's written permission.

No Amendment Except in Writing

This license may not be amended except in a writing signed by both parties (or, in the case of Springer, by CCC on Springer's behalf).

Objection to Contrary Terms

Springer hereby objects to any terms contained in any purchase order, acknowledgment, check endorsement or other writing prepared by you, which terms are inconsistent with these terms and conditions or CCC's Billing and Payment terms and conditions. These terms and conditions, together with CCC's Billing and Payment terms and conditions (which are incorporated herein), comprise the entire agreement between you and Springer (and CCC) concerning this licensing transaction. In the event of any conflict between your obligations

established by these terms and conditions and those established by CCC's Billing and Payment terms and conditions, these terms and conditions shall control.

Jurisdiction

All disputes that may arise in connection with this present License, or the breach thereof, shall be settled exclusively by arbitration, to be held in the Federal Republic of Germany, in accordance with German law.

Other conditions:

V 12AUG2015

Questions? customercare@copyright.com **or +1-855-239-3415 (toll free in the US) or +1-978-646-2777.**

Dear Navipedia Editors,

My name is David P. Schafer. I am a graduate student in the Master of Science in Engineering program at the Milwaukee School of Engineering in Milwaukee, Wisconsin. I am in the process of completing my Master's Capstone Report entitled, "Examining Forces at Geostationary Orbit with Galaxy 15 Uncontrolled Wide Area Augmentation System Ephemerides"

I am requesting permission to use material for which Navipedia holds the copyright. Specifically, I am requesting permission to use the following copyright-protected material in my capstone report:

[1] *Figure 1: Perturbations over the Satellite Orbit* on the *Perturbed Motion* webpage at: http://www.navipedia.net/index.php/Perturbed_Motion

Three copies of [1] above are to be placed in three paper copies of my capstone report. One paper copy of the capstone report will be placed in the Electrical Engineering department file; one paper copy of the capstone report will be kept in the Thesis Archives which has no public access; and one paper copy of the capstone report will be placed in the library where interested patrons can check it out.

In addition, an electronic copy of my capstone report will be made available on the Milwaukee School of Engineering Library's website.

If you have any questions, please feel free to contact me at [   ] or via e-mail at [   ]

Thank you,
David P. Schafer

The previous letter was submitted to the editors of the webpage Navipedia on October 9th, 2016. No response was received.

Engineering

Capstone Report Approval Form

Master of Science in Engineering – MSE

Milwaukee School of Engineering

This capstone report, titled "Examining Forces at Geostationary Orbit with Galaxy 15 Uncontrolled Wide Area Augmentation System Ephemerides," submitted by the student David P. Schafer, has been approved by the following committee:

Faculty Co-Advisor: _____   Date: _____

Dr. Jill Seubert, Ph.D.

Faculty Co-Advisor: _____   Date: _____

Dr. Subha Kumpaty, Ph.D.

Faculty Member: _____   Date: _____

Professor Gary Shimek, M.L.I.S.